UNIVERSIDADE ESTADUAL DE CAMPINAS

FACULDADE DE ENGENHARIA QUÍMICA

DANIEL PEREIRA SACOMANI

INFLUÊNCIA DO TEMPOL NA ESTABILIDADE DE HIDROGÉIS DE ÁCIDO HIALURÔNICO SOB *STRESS* OXIDATIVO PARA APLICAÇÕES EM ORTOPEDIA REGENERATIVA

THE INFLUENCE OF TEMPOL ON THE STABILITY OF HYALURONIC ACID UNDER OXIDATIVE STRESS FOR REGENERATIVE ORTHOPEDICS APPLICATIONS

CAMPINAS

2019

DANIEL PEREIRA SACOMANI

INFLUÊNCIA DO TEMPOL NA ESTABILIDADE DE HIDROGÉIS DE ÁCIDO HIALURÔNICO SOB *STRESS* OXIDATIVO PARA APLICAÇÕES EM ORTOPEDIA REGENERATIVA

THE INFLUENCE OF TEMPOL ON THE STABILITY OF HYALURONIC ACID UNDER OXIDATIVE STRESS FOR REGENERATIVE ORTHOPEDICS APPLICATIONS

Dissertação apresentada à Faculdade de Engenharia Química da Universidade Estadual de Campinas como parte dos requisitos exigidos para obtenção do título de mestre em Engenharia Química.

Dissertation presented to the School of Chemical Engineering of the University of Campinas in partial fulfillment of the requirements for the degree of Master, in the area of Chemical Engineering.

Profª Drª Maria Helena Andrade Santana

Orientadora

Este exemplar corresponde à versão final da dissertação defendida pelo aluno Daniel Pereira Sacomani orientado pela Prof.ª Dr.ª Maria Helena Andrade Santana.

CAMPINAS

2019

Agência(s) de fomento e nº(s) de processo(s): CNPq, 153611/2016-2

Ficha catalográfica
Universidade Estadual de Campinas
Biblioteca da Área de Engenharia e Arquitetura
Rose Meire da Silva - CRB 8/5974

Sa14i

Sacomani, Daniel Pereira, 1991-
Influência do tempol na estabilidade de hidrogéis de ácido hialurônico sob stress oxidativo para aplicações em ortopedia regenerativa. / Daniel Pereira Sacomani. – Campinas, SP : [s.n.], 2019.

Orientador: Maria Helena Andrade Santana.
Dissertação (mestrado) – Universidade Estadual de Campinas, Faculdade de Engenharia Química.

1. Tempol. 2. Ácido hialurônico. 3. Estresse oxidativo. I. Santana, Maria Helena Andrade, 1951-. II. Universidade Estadual de Campinas. Faculdade de Engenharia Química. III. Título.

Informações para Biblioteca Digital

Título em outro idioma: The influence of tempol on the stability of hyaluronic acid under oxidative stress for regenerative orthopedic applications.
Palavras-chave em inglês:
Tempol
Hyaluronic acid
Oxidative stress
Área de concentração: Engenharia Química
Titulação: Mestre em Engenharia Química
Banca examinadora:
Maria Helena Andrade Santana [Orientador]
Denise Gradella Villalva
Marcos Akira D'Ávila
Data de defesa: 20-02-2019
Programa de Pós-Graduação: Engenharia Química

Folha de Aprovação da Dissertação de mestrado defendida por Daniel Pereira Sacomani e aprovada em 20 de fevereiro de 2019 pela banca examinadora constituída pelos doutores:

Profª. Drª. Maria Helena Andrade Santana - Presidente
FEQ – UNICAMP

Drª. Denise Gradella Villalva
Consiglio Nazionale dele Ricerche

Prof. Dr. Marcos Akira D'Ávila
FEM - UNICAMP

*A Ata de Defesa com as respectivas assinaturas dos membros encontra-se no SIGA/Sistema de Fluxo de Tese e na Secretaria do Programa da Unidade.

AGRADECIMENTOS

Agradeço à Professora Maria Helena Andrade Santana pela orientação, incentivo e confiança no meu trabalho ao longo da minha pesquisa.

Agradeço também ao Gilson, membro indispensável no LDPB, por estar sempre disposto a ajudar a todos e ser um grande colega.

A todos meus colegas de laboratório, sobretudo Bruna, Fabiane, Maria Paula, Carla e Luane por terem sido peças essências no desenvolvimento desta pesquisa.

À Drª Denise Gradella Villalva e ao Prof Dr Marcos Akira D'Ávila por terem feito parte da banca examinadora e pelas valiosas considerações.

À minha família, principalmente meu pai, minha mãe, meu irmão, por todo o suporte dado ao longo de minha vida.

A meus amigos, Evan, Guilherme, Maria Fernanda, Carol, Nadia, Natália, Ana, Felipe e Ivan, pelo companheirismo e suporte emocional.

Finalmente, ao CNPq pelo suporte financeiro.

RESUMO

O ácido hialurônico (AH) de alta massa molar tem sido usado tanto como viscossuplemento quanto como *scaffold* para células tronco e/ou fatores de crescimento no tratamento de doenças das articulações. Entretanto, uma das principais limitações de seu uso *in vivo* é a sua baixa estabilidade na presença de espécies reativas de oxigênio (ROS). A oxidação promovida por esses radicais resulta na cisão das cadeias do AH, redução de sua massa molar, desestabilização de sua estrutura coloidal e comprometimento de sua atividade biológica. Estratégias comumente usadas para estabilização do AH envolvem reticulação química, derivatização com moléculas antioxidantes ou associação com macromoléculas protetoras de superfície. Nesse contexto, o presente trabalho estudou a estabilização do AH por meio de sua oxidação parcial com periodato, reticulação química com dihidrazida adípica (ADH) e incorporação do antioxidante tempol para aplicações em ortopedia regenerativa. Inicialmente as alterações estruturais decorrentes da produção do AH oxidado (oxi-AH) foram caracterizadas por meio de propriedades tais como grau de oxidação, viscosidade, diâmetro hidrodinâmico e potencial zeta, modulação da reticulação química com ADH e capacidade de incorporação e liberação gradual do tempol. Na segunda etapa, foi estudada a estabilidade sob *stress* oxidativo de hidrogéis de oxi-AH preparados a partir dos graus de oxidação 44 ± 4, 65 ± 5, 82 ± 5 % e concentrações de ADH 2, 4 e 8 % configurados em géis sólidos planos e incorporando 5 mg de tempol. Adicionalmente os hidrogéis de oxi-AH (grau de oxidação 65 ± 5 % e ADH 8%) foram configurados em micro e nanopartículas que incorporaram 7,4 ± 0,7 e 11 ± 3 de g de tempol/g de partícula, respectivamente, com o objetivo de serem adicionadas aos hidrogéis de configuração plana, visando maior estabilidade. Perfis de degradação dos hidrogéis em função do tempo foram construídos a partir da perda de massa sob *stress* oxidativo produzido pelo peróxido de hidrogênio (100 µmol/L.). A degradação em tampão PBS foi usada como controle. Os resultados mostraram que as mudanças estruturais nos hidrogéis de oxi-AH foram favoráveis à sua injetabilidade, favorecendo a incorporação do tempol e a sua reticulação *in situ,* e a presença de tempol aumentou a resistência contra o *stress* oxidativo comparados aos controles, com manutenção da integridade hidrogéis entre 2 e 22 dias dependendo da composição oxi-AH/ADH. Este trabalho apresenta resultados inovadores em termos de formulações de AH, que são úteis aplicações em medicina regenerativa.

ABSTRACT

High molar mass hyaluronic acid (HA) has been used as a viscossuplement and as a scaffold for stem cells and/or growth factors in the treatment of joint diseases. However, the low stability in the presence of reactive species of oxygen (ROS) is the main limitation of HA in vivo uses. The oxidation promoted by these free radicals results in the degradation of AH's chains, decrease of its molar mass, changes in its colloidal domain and compromising of its biological functions. Some of the most common strategies used in the stabilization of AH are chemical crosslinking, derivatization with antioxidant molecules or association with surface protective molecules. In this context, the present work studied the stabilization of high molar mass AH after its oxidation with periodate, subsequent chemical crosslinking with adipic acid dihydrazide (ADH) and incorporation of the antioxidant tempol for applications in regenerative medicine. Initially, the changes caused in AH during the production of oxidized HA (oxi-HA) were studied by analyzing properties such as degree of oxidation, viscosity, hydrodynamic diameter and zeta potential and capacity of tempol incorporation. Secondly, the stability under oxidative stress of hydrogels made with oxi-HA whose degrees of oxidation were 44 ± 4, 65 ± 5, 82 ± 5 % and ADH concentration of 2, 4 e 8 %, in which 5 mg de tempol were incorporated. Besides that, hydrogels (degree of oxidation 65 ± 5 % and ADH 8%) were configured as micro and nanoparticles, which incorporated 7,4 ± 0,7 e 11 ± 3 g of tempol/g of particles in order to add them in the hydrogels. Degradation profiles were constructed using the loss of each hydrogel mass under oxidative stress, induced by 100 µmol/L hydrogen peroxide solution. The degradation in PBS buffer was used as control. The results show the structural changes in the oxi-HA were in favor of its injectability, favoring its in situ crosslinking. The presence of tempol increased the hydrogels against the oxidative stress in comparison with the controls, which increased the hydrogel's integrity between 2 and 22 days depending on the composition. This work presents data that promotes the technological innovation of AH's usage in regenerative medicine.

LISTA DE FIGURAS

LISTA DE TABELAS

LISTA DE ABREVIAÇÕES E SIGLAS

Sigla	Significado
ABTS	*(2,2'-Azino-bis(3-ethylbenzthiazoline-6-sulfonic acid))*
ADH	Dihidrazida adípica
AH	Ácido hialurônico
AR	Artrite reumatóide
BDDE	4-Butanediol diglicidil éter
DLS	*Dynamic light scattering*
DO	Densidade ótica
DPPH	*2,2-Diphenyl-1-picrylhydrazyl*
DVS	Divinil sulfona
ECM	Matriz extracelular
FTIR	Infravermelho com Transformada de Fourier
HA	*Hyaluronic acid*
HPLC	High performance liquid chromatography
MEV/SEM	Microscópio eletrônico de varredura
MM	*Molar mass*
OA	Osteoartrite
OCDE	Organização para a Cooperação e Desenvolvimento Económico
Oxi-AH	Ácido hialurônico oxidado
Oxi-HA	*Oxidized hyaluronic acid*
PBS	*Phosphate buffered saline*
PDI	*Polydispersity index*
PEG	Polietilenoglicol
PLA	Ácido polilático
PLGA	Ácido polilático-glicólico
PGA	Ácido poliglicólico
ROS	Espécies reativas de oxigênio
t-BC	Terc-butilcarbazato
TNBS	2,4,6-trinitrobenzeno sulfônico

SUMÁRIO

1. INTRODUÇÃO

Com o aumento da expectativa de vida e o envelhecimento da população mundial, surge uma série de preocupações referentes à saúde humana que anteriormente não eram consideradas ou não recebiam tanta atenção. Essas questões podem ser referentes à estética, como preenchimentos dérmicos para suavizar os efeitos da idade, ou à saúde, como tratamentos de condições relacionadas ao desgaste das estruturas físicas do organismo humano (IANNITTI et al., 2013).

De acordo com dados da Organização para a Cooperação e Desenvolvimento Económico (OCDE) os gastos de verba pública destinados à assistência médica aumentam consideravelmente dependendo da faixa etária da população, como é possível observar pela Figura 1. Esse fenômeno ocorre principalmente pela perda da capacidade de regeneração do organismo humano com o avanço da idade e o surgimento de doenças e lesões crônicas (MARTINS, 2013).

Figura 1. Gastos públicos destinados à saúde por faixa etária. Modificado de Martins (2013).

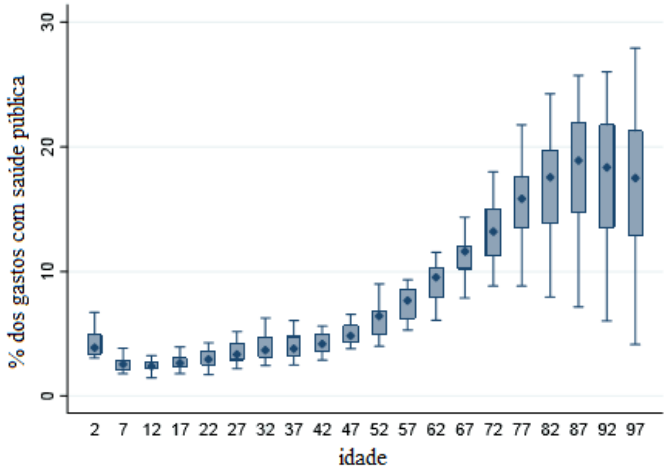

O organismo humano possui uma capacidade limitada de regeneração de órgãos e tecidos, sobretudo quando estão presentes lesões importantes, disfunções no organismo, doenças autoimunes e desgastes naturais decorrentes do envelhecimento. É nesse contexto que se inserem a medicina regenerativa, a engenharia de tecidos e os biomateriais. Esses ramos de interface entre a medicina e a engenharia têm por objetivos desenvolver estratégias para a acelerar o potencial do organismo humano de auto regeneração. De maneira geral, essas

técnicas tentam mimetizar os mecanismos de reparação natural do organismo e regular a fisiologia da região afetada (CHEN; LIU, 2016).

Quando uma estrutura do organismo humano sofre um ferimento, uma cascata de respostas biológicas ocorre com o intuito de recuperá-la, entretanto, dependendo de sua gravidade são necessárias intervenções cirúrgicas (tratamentos convencionais), ou tratamentos não-cirúrgicos. Dentro da engenharia de tecidos, existem três pilares essenciais para a regeneração de estruturas: *scaffolds*, células tronco e sinais regulatórios. A Figura 2 apresenta um esquema dos três pilares essenciais para a engenharia de tecidos (MURPHY et al., 2013; QAZI et al., 2015).

Figura 2. Os três pilares essenciais para a engenharia de tecidos. Modificado de Murphy et al. (2013).

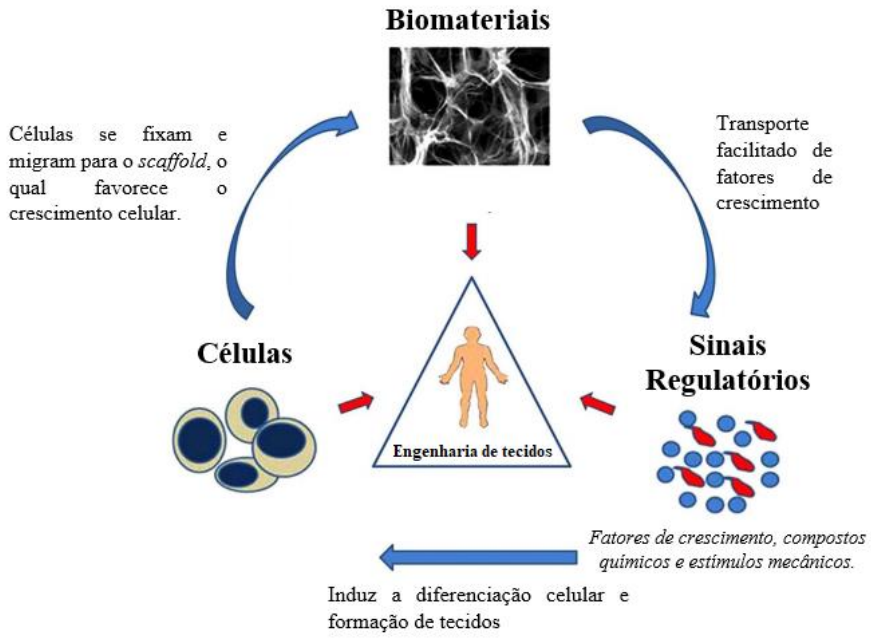

Na engenharia de tecidos, no estudo da recuperação de cartilagem, são utilizadas comumente células tronco mesenquimais. Essas células possuem a capacidade de se diferenciar em diferentes tipos de células, como células de cartilagem, gordura, músculo, etc. Uma das vantagens da associação desse tipo de célula com *scaffolds* é a possiblidade da cultura se desenvolver em três dimensões, aumentando a interação entre as células mimetizando a matriz extracelular (ECM) de maneira mais satisfatória do que uma cultura em duas dimensões (LI et al., 2005).

O principal papel dos *scaffolds* é guiar o processo de regeneração. Eles podem ser constituídos de materiais sintéticos ou naturais, cujo papel é mimetizar a ECM e então promover migração, crescimento e diferenciação celular. Além de fornecer uma estrutura para o crescimento celular, o *scaffold* pode servir também de substrato para os novos tecidos em formação (MURPHY et al., 2013; QAZI et al., 2015).

Para que um *scaffold* seja capaz de ser eficaz no processo de regeneração de tecidos, são necessários que alguns requerimentos biológicos, mecânicos e anatômicos sejam atingidos. Do ponto de vista biológico, características importantes como o tamanho de poro, estrutura da superfície do substrato, rugosidade e hidrofilicidade são algumas das características que influenciam diretamente a migração e adesão celular (LEONG et al., 2008).

Do ponto de vista mecânico, o *scaffold* deve possuir força mecânica suficiente a ponto de manter sua estrutura e possuir espaço para o transporte de células e nutrientes. Além disso, as propriedades mecânicas do *scaffold* devem ser compatíveis com as propriedades mecânicas da região em que esse material vai ser introduzido. Anatomicamente, o *scaffold* deve possuir o mesmo tamanho e formato da região no qual ele será inserido. Isso fará com o que sua fixação ocorra de maneira satisfatória (LEONG et al., 2008).

O desenvolvimento desse tipo de tecnologia permite um controle maior sobre as redondezas das células, fazendo com que ele se assemelhe mais ao ambiente promovido pela ECM. Para que essas características sejam alcançadas é interessante que o scaffold seja bioativo, ou seja, um material cuja estrutura estimule determinadas funções celulares. A Figura 3 apresenta um diagrama representando a relação entre células e *scaffolds*. (EVANS; GENTLEMAN; POLAK, 2006).

Figura 3. Diagrama representado a relação entre células e *scaffolds*. Modificado de Evans, Gentleman & Polak (2006).

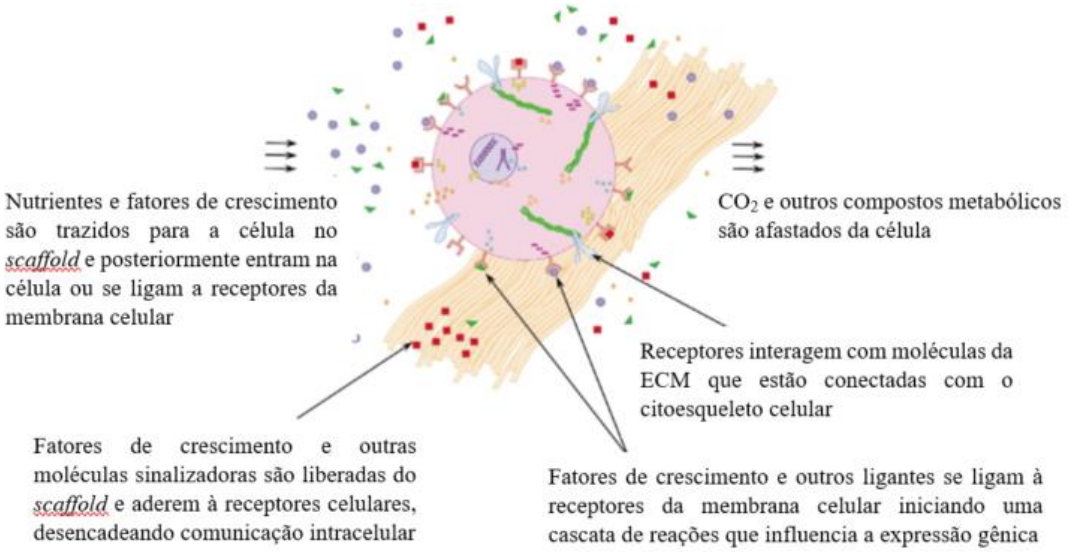

Dentre os materiais comumente utilizados para a fabricação de *scaffolds*, os materiais sintéticos apresentam a vantagem de sua estrutura, formato e composição serem facilmente alterados de maneira que o *scaffold* se assemelhe à ECM. Os polímeros sintéticos utilizados com maior frequência para regeneração de tecidos são: ácido polilático (PLA), ácido poliglicólico (PGA), ácido polilático-glicólico (PLGA) e polietilenoglicol (PEG). Apesar desses materiais serem biocompatíveis e não promoverem nenhuma resposta inflamatória expressiva no organismo, eles não possuem funções biológicas e não são capazes de interferir na sinalização celular, o que pode dificultar a proliferação celular (CHEN; LIU, 2016).

Uma alternativa aos materiais sintéticos são os biomateriais derivados de fontes naturais, sobretudo por apresentarem bioatividade, biocompatibilidade e estrutura semelhante à ECM. Durante seu processo de produção industrial, esses biomateriais frequentemente são produzidos na ausência de solventes orgânicos tóxicos e, durante sua degradação no organismo, não liberam materiais citotóxicos de maneira expressiva. Outra vantagem da utilização desses biomateriais é sua capacidade de promover respostas biológicas, as quais promovem adesão e proliferação celular. Colágeno, alginato e quitosana são exemplos desse tipo de material comumente utilizados (CHEN; LIU, 2016).

Dentre os biomateriais tradicionais, destaca-se o ácido hialurônico, sobretudo pelo fato de sua biocompatibilidade e de sua capacidade de induzir a proliferação e diferenciação celular. Entretanto, quando utilizado como viscossuplemento, o AH tem um tempo de

permanência baixo no organismo humano, por isso foram desenvolvidas algumas estratégias para que esse problema fosse contornado (GARG; HALES, 2004; LAI et al., 2016).

Uma das estratégias utilizadas para retardar a degradação do AH é a reticulação química, a qual modifica a estrutura do material, sem que ocorra a perda expressiva de sua função biológica, preservando sua biocompatibilidade e aumentando o tempo de permanência no organismo.

Os reticulantes químicos mais usados inclusive em produtos comerciais, são a divinil sulfona (DVS) e o 1,4 butanediol diglicil éter (BDDE). Um dos agentes reticulantes que apresenta características interessantes para aplicações médicas é a dihidrazida adípica (ADH), sobretudo por ser metabolizado pelo organismo humano.

A reticulação convencional de AH com ADH envolve a utilização de catalisadores, os quais devem ser retirados em processos de purificação posteriores à reticulação (GARG; HALES, 2004; PAN et al., 2013).

Uma das maneiras de ser contornar a utilização de catalisadores na reticulação do AH com ADH é a oxidação do AH. A abertura de um dos anéis do polímero gera grupos aldeído, os quais reagem com ADH sem gerar subprodutos tóxicos. Outra vantagem da oxidação do AH é sua baixa viscosidade e a possibilidade de injeção e gelificação *in situ* (GARG; HALES, 2004).

Neste trabalho, hidrogéis incorporando tempol em matrizes de oxi-AH reticuladas com ADH foram preparados e caracterizados quanto à influência do grau de oxidação do AH nas suas propriedades físico-químicas, liberação modificada do tempol e estabilidade sob stress oxidativo.

2. OBJETIVO E METAS

O presente trabalho teve como objetivo estudar a influência do grau de oxidação do AH na preparação de hidrogéis reticulados com ADH e incorporando tempol, e na sua estabilidade sob stress oxidativo.

O desenvolvimento deste trabalho foi composto das seguintes metas:

- Produção e caracterização de AH parcialmente oxidado (oxi-AH) com três graus de oxidação;
- Influência do oxi-AH na capacidade de liberação do tempol em hidrogel reticulado com ADH;
- Preparar e caracterizar hidrogéis de oxi-AH/ADH contendo tempol nas configurações sólida, e de micro e nanopartículas;
- Estudo da estabilidade de hidrogéis de oxi-AH/ADH sob stress oxidativo induzido por peróxido de hidrogênio e em tampão fosfato.

3. REVISÃO BIBLIOGRÁFICA

3.1. Ácido hialurônico.

3.1.1. Histórico e propriedades.

O ácido hialurônico é um polissacarídeo natural, linear, composto de unidades alternadas de ácido d-glucurônico e n-acetilglicosamina, unidas por ligações β-1,3 e β-1,4. Pertencente ao grupo dos glicosaminoglicanos, o AH possui estrutura diferenciada por ser a única molécula dessa família que não é sulfatado nem possui peptídeos. O AH está naturalmente presente nos tecidos conjuntivos de mamíferos em concentrações que variam de 4 g/kg no cordão umbilical, 2 a 4 g/L no fluido sinovial e 0,2 g/kg na derme. A maior quantidade de AH no organismo humano é encontrada na matriz intracelular da pele e de tecidos musculoesqueléticos (GARG; HALES, 2004).

O AH foi identificado pela primeira vez em 1934 quando Karl Meyer e John Palmer estudavam o humor vítreo de bois, substância presente no interior do globo ocular. Por apresentar ácido urônico e ser encontrado no globo ocular, a substância foi nomeada ácido hialurônico ("hyaloid" = vítreo + ácido urônico). Durante as décadas posteriores, a molécula de AH foi isolada de várias fontes, como o cordão umbilical, crista de galos e bactérias do gênero Streptococcus (LIU et al., 2011; MEYER; PALMER, 1934). A Figura 1 apresenta uma microscopia de uma célula humana da mucosa bucal e fibras de AH ao seu redor.

Figura 1. Microscopia indicando três tipos de fibras de AH ao redor de uma célula humana de mucosa bucal. Retirado de Garg & Hales (2004).

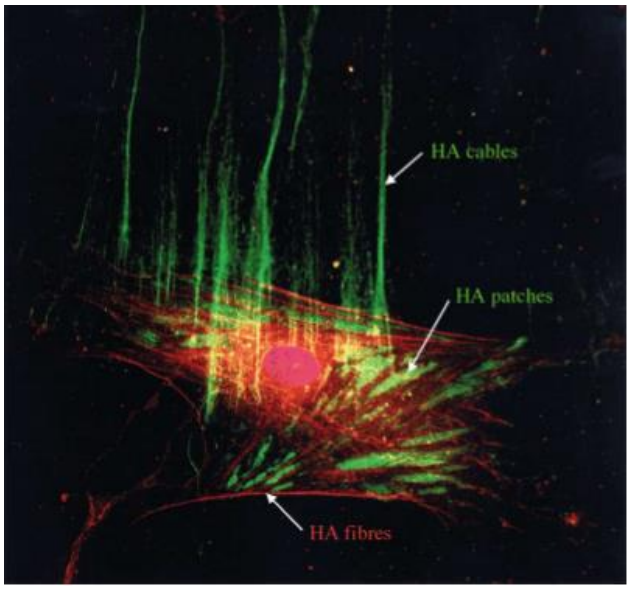

O AH possui uma ampla faixa de massa molar (10^4 - 10^7 Da) devido às suas diferentes funções no organismo humano. O AH de baixa massa molar é envolvido nos mecanismos de sinalização molecular, enquanto que o de alta massa molar, exerce a função lubrificante, reduzindo o atrito entre as cartilagens das articulações durante o movimento. (GARG; HALES, 2004).

3.1.2. Ácido hialurônico em solução.

Em solução fisiológica a molécula do AH ocupa um volume altamente hidratado com estrutura de fitas torcidas, devido à presença de domínios hidrofílicos e hidrofóbicos (GARG; HALES, 2004). Em soluções semidiluídas ou concentradas a estrutura do AH é estabilizada graças ao *crosslinking* físico (MALEKI; KJØNIKSEN; NYSTRÖM, 2008). A Figura 2 mostra as estruturas primária e secundária do AH.

Figura 2. Estrutura molecular do AH onde os átomos de hidrogênio representam as faces hidrofóbicas. Retirado de Garg & Hales (2004).

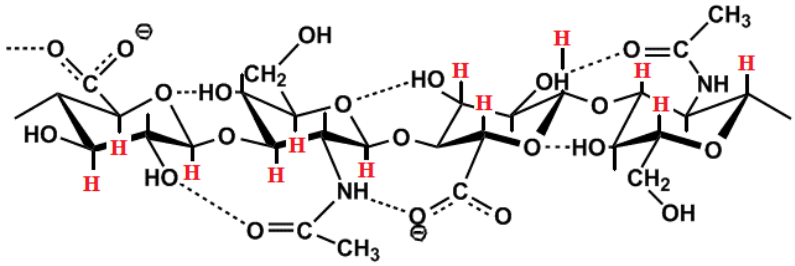

Soluções contendo moléculas de AH em concentrações maiores que 0,1 mg/L possuem propriedade elásticas e viscosas. O intercâmbio dessas propriedades faz com que o AH seja um fluido natural capaz de, a baixas frequências (abaixo de 0,1 Hz) fazer a transição de um fluido viscoso para um fluido viscoelástico, ou seja, um fluido que, ao sofrer deformações, são deformados viscosamente e elasticamente. As deformações viscosas ideias são definidas como contínuas e irreversíveis sob uma tensão de cisalhamento, também chamadas de escoamento. Já as deformações elásticas ideias são definidas como reversíveis, ou seja, ao fim da aplicação da tensão, o material volta para a forma e dimensões originais. Dessa maneira, quando o organismo humano se encontra em repouso, há baixa tensão de cisalhamento e o AH é viscoso e, assim que o corpo inicia o movimento, ocorre um aumento na tensão de cisalhamento e o AH torna-se viscoelástico, conferindo lubrificação para as articulações e facilitando o movimento (HASCALL; LAURENT, 1997).

Essa mudança de propriedades acontece à baixa energia em pessoas jovens e saudáveis, entretanto, com o envelhecimento do indivíduo, surgimento de doenças articulares e lesões, começam a ocorrer processos de degradação do fluido sinovial e do AH os quais fazem com que seja necessário um gasto maior de energia para que o movimento das juntas seja executado (HASCALL; LAURENT, 1997).

Quando em solução, dependendo de fatores como concentração e pH, as moléculas de AH podem se organizar em diversas conformações, como *rigid rod* e *random coil*, essa última sendo uma organização em que as moléculas se dispões aleatoriamente umas sobre as outras, sem nenhum formato definido. Em baixas concentrações e pH fisiológico essa é a conformação mais comum nas moléculas de AH (HASCALL; LAURENT, 1997; HOKPUTSA et al., 2003; INGR; KUTÁLKOVÁ; HRNČIŘÍK, 2017). A Figura 3 representa o AH na conformação *random coil.*

Figura 3. Representação do AH na conformação *random coil*.

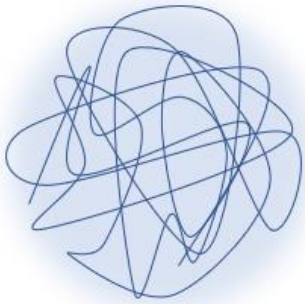

3.1.3. Produção industrial e aspectos econômicos.

O AH pode ser extraído de partes de animais, como a crista de galo, ou via fermentação bacteriana. Na crista de galo, o AH encontra-se complexado com proteoglicanos, o que faz seu isolamento e purificação terem custos altos (CHONG et al., 2005; REGAN et al., 1994). Do ponto de vista industrial, ecológico e farmacêutico, essa não se trata da melhor opção. Além da quantidade expressiva de resíduos produzidos, há a possibilidade de que proteínas e patógenos não sejam retirados durante a purificação, os quais gerariam respostas indesejadas no organismo do paciente (LIU et al., 2011; NECAS et al., 2008).

O HA é sintetizado como uma capsula extracelular por algumas bactérias do gênero Streptococcus. Essas bactérias apresentam formato esférico e podem se organizar em duplas ou em grupos maiores. Estipula-se que essa capsula de AH sirva como mecanismo protetor dessas

bactérias, impedindo que sua presença em um organismo seja reconhecida pelo sistema imunológico como um corpo estranho e protegendo as bactérias da ação de substâncias produzidas por células de defesa. Estipula-se também que a camada de AH facilite a mobilidade dessas bactérias pelo tecido epitelial de animais (CLEARY; LARKIN, 1979) A Figura 4 apresenta uma micrografia eletrônica de bactérias do gênero Streptococcus envoltas por cápsulas de AH.

Figura 4. Micrografia eletrônica de bactérias do gênero Streptococcus. Modificado de Chong et al. (2004).

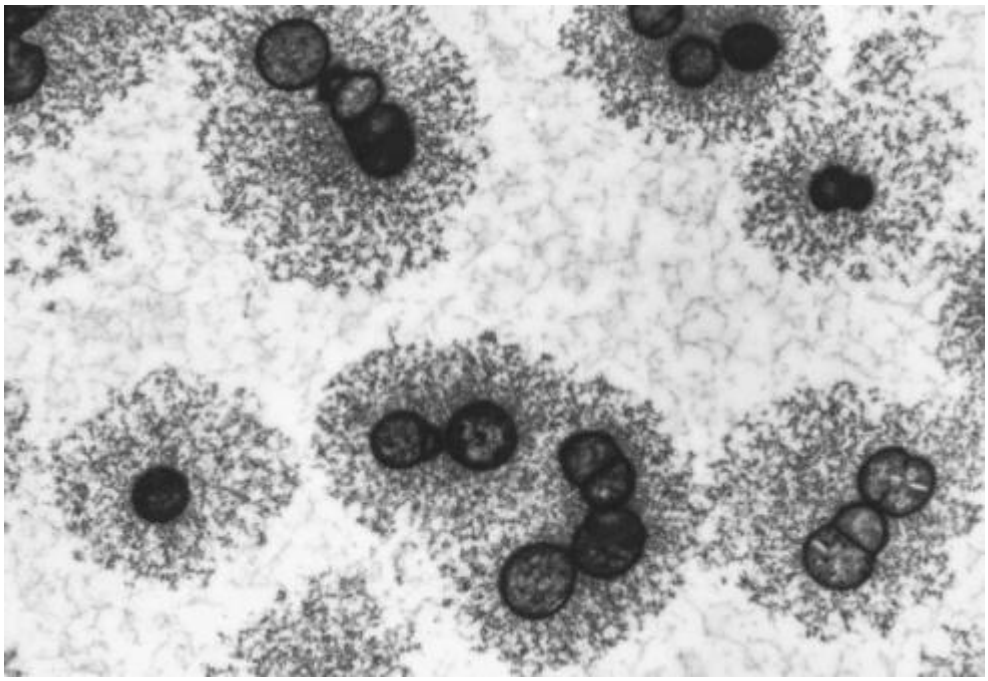

Atualmente, devido aos avanços da engenharia genética, grandes esforços foram destinados para produção de AH por meio de DNA recombinante. Há registros de tentativas de produção de AH com auxílio de bactérias Bacillus sp., L. lactis, Agrobacterium sp. e. coli. Apesar de estar disponível no mercado, o AH recombinante não ocupa um espaço tão relevante quanto o AH produzido por gênero Streptococcus sp (LIU et al., 2011).

O AH de alta pureza e massa molar é um produto de alto valor agregado, com previsão para ocupar um importante papel no grupo dos biomateriais utilizados para tratamento ortopédico, os quais movimentaram 5,8 bilhões de dólares em 2010 de acordo com iDataResearch Inc (2010). Em 2016, de acordo com Grand View Research (2016), o mercado

global de AH foi estipulado em 7,2 bilhões de dólares, com previsão de aumento nos anos seguintes.

Parte desse mercado é incentivado pelo aumento da procura por tratamentos estéticos não invasivos. Ainda de acordo com Grand View Research (2016), em 2015 a população americana gastou mais de 5 bilhões de dólares em procedimentos cosméticos, nesse contexto o número de injeções de AH encontram somente abaixo de injeções de botox. Em 2014, foram feitos aproximadamente 1,8 milhões de procedimentos desse tipo somente nos Estados Unidos.

De acordo com Grand View Research (2016). As principais empresas produtoras de AH para fins médicos e cosméticos são Allergan, Inc.; Sanofi (Genzyme); Salix Pharmaceuticals; Seikagaku Corporation; Galderma S.A., Zimmer Holdings, Inc.; Smith & Nephew Plc; Ferring Pharmaceuticals, Inc.; Anika Therapeutics, Inc.; e F. Hoffmann-La Roche Ltd.

3.1.4. Aplicações médicas e cosméticas.

Devido às suas características, sobretudo viscoelasticidade, biocompatibilidade e não imunogenicidade, o AH é utilizado em diversas aplicações clínicas, como suplementação do fluido sinovial, também conhecido como viscossuplementação, ou preenchimentos cosméticos

3.1.4.1. Cosmética

O AH é um importante biomaterial para a indústria cosmética considerando que mais de 50 % do AH encontrado no corpo humano encontra-se na derme e epiderme. O AH é utilizado em produtos destinados a combater o ressecamento e perda de elasticidade da pele associada ao envelhecimento. Ele é comumente utilizado na formulação de cosméticos denominados anti-idade devido às suas propriedades hidratantes e viscoelásticas. O primeiro produto estético comercializado utilizando AH foi um creme para tratamento de queimaduras e úlceras - HYALGAN (Itália, 1960) (CHONG et al., 2005; PAN et al., 2013).

3.1.4.2. Aplicações oftalmológicas

Por ser um componente natural do humor vítreo, o AH é um excelente candidato para aplicações oftalmológicas. Durante cirurgias, a injeção intraocular de AH serve para manter o formato da câmara anterior do olho, região entre a superfície posterior da córnea e a íris (NECAS et al., 2008)

AH também é aplicado em conjunto com hialuronidase, anestésicos e outros medicamentos em algumas cirurgias oftalmológicas. A hialuronidase reduz a massa molar do AH, facilitando sua permeação pelos tecidos oculares, fazendo com as moléculas de fármacos também sejam dispersadas em conjunto (NECAS et al., 2008).

Uma outra aplicação oftalmológica de AH é a patente de Lin et al. (2011) a qual descreve a produção de um hidrogel baseado na oxidação de AH e sua reticulação para uso como substituto do humor vítreo do olho humano. Devido a suas características como baixa viscosidade e consequente potencial de injetabilidade, baixa toxicidade e transparência, esse material apresenta uma promissora possibilidade para esse tipo de aplicação.

3.1.4.3. Viscossuplementação

Graças à sua natureza viscoelástica, o AH é capaz de formar matrizes altamente hidratadas, agindo como um lubrificante e amortecedor nas articulações, entretanto, na presença de determinadas patologias, as cadeias de AH sofrem alterações que promovem a perda de viscoelasticidade. Essas alterações são resultado de diminuição de massa molar e concentração no fluido sinovial. É nesse contexto que surge o conceito de viscossuplementação, ou seja, a injeção de AH exógeno a fim de se restaurar as propriedades mecânicas do fluido sinovial (BALAZS; DENLINGER, 1993; WATTERSON; ESDAILE, 2000).

3.1.5. O fluido sinovial e doenças inflamatórias.

O fluido sinovial é um fluido presente nas articulações do corpo humano cujas principais funções são lubrificação e amortecimento. O fluido sinovial é constituído majoritariamente de quatro componentes: AH, albumina, mucinas (glicoproteínas de alta massa molar) e globulina. Cada uma dessas moléculas desempenha uma função diferente, sendo o AH responsável pelo aumento da viscosidades em baixas taxas de cisalhamento (GHOSH et al., 2014; RINAUDO et al., 2014).

Quando há a degradação do fluido sinovial graças a doenças inflamatórias, injeções de AH de alta massa molar podem ser utilizadas como viscossuplementos, entretanto esse tipo de tratamento não possuiu a capacidade de restaurar qualquer estrutura comprometida, atuando somente na lubrificação da junta e na redução da dor (RINAUDO et al., 2014).

Dentre as doenças inflamatórias das articulações, destaca-se a osteoartrite (OA), uma desordem crônica que acomete principalmente a população idosa, sendo caracterizada pela inflamação e deformação nas juntas. Essa degeneração resulta em dor e na limitação de movimentos, como andar e subir escadas e, em casos mais extremos, faz-se necessária a

substituição completa do quadril ou do joelho afetados. Estudos mostram que a OA se manifesta mais comumente em pessoas acima dos 50 anos e de maneira diferente de acordo com os sexos: homens são os mais afetados quando mais jovens, porém, após os 50 anos as mulheres tornam-se as mais acometidas nas mãos, joelhos e pés (CROSS et al., 2014; MODAWAL et al., 2005). A Figura 5 apresenta o esquema de uma articulação comprometida com OA (DOUGADOS et al., 2014).

Figura 5. Esquema de uma junta comprometida com osteoartrite. Modificado de Arden et al. (2014).

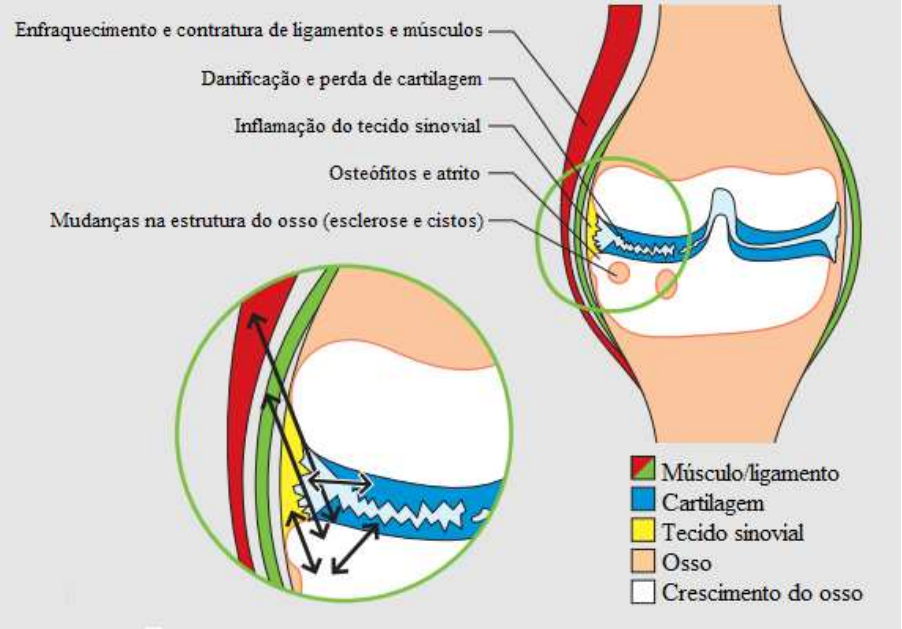

Atualmente existem tratamentos cirúrgicos e não-cirúrgicos capazes de amenizar os sintomas e tratar os estágios finais da OA, entretanto trata-se de uma condição sem cura. Isso faz com que os pacientes que convivem com essa condição percam qualidade de vida e tenham chances aumentadas de desenvolver problemas psicológicos e tenham sua vida profissional afetada negativamente (PALMIERI-SMITH et al., 2017).

Outra alteração importante nas juntas é a artrite reumatóide (AR), a atrite inflamatória autoimune mais comum em adultos. Assim como a OA, essa condição dificulta a realização de tarefas domésticas e relacionadas ao trabalho, impactando seriamente a qualidade de vida dos pacientes. A AR provoca dores e degeneração de órgãos além da cartilagem, como coração, pulmão e vasos sanguíneos. Em casos extremos, há alterações no fluido sinovial do paciente, o qual torna-se rico em neutrófilos, células do sistema imunológico presentes em

inflamações, o que altera a homeostase do conjunto, ou seja, o equilíbrio necessário para que o organismo realize suas funções corretamente (ŠOLTÉS et al., 2006).

O tratamento da AR sofreu modificações durante as últimas décadas graças ao desenvolvimento de novas tecnologias, entretanto essa condição ainda exige estudos para que tratamentos mais eficazes surjam.

3.1.6. Modificações químicas no AH.

No organismo de mamíferos, existem três enzimas responsáveis pela degradação do AH: hialuronidase, b-d-glucuronidase, e β-Nacetil-hexosaminidase. A ação da hialuronidase faz com que moléculas de AH com alta massa molar sejam transformadas em oligômeros menores enquanto a b-d-glucuronidase, e β-Nacetil-hexosaminidase continuam a degradação desses oligômeros removendo frações terminais não reduzíveis. Essa redução expressiva de massa molar é responsável pelo aumento na permeabilidade do AH pelos tecidos do organismo (LEACH; SCHMIDT, 2004).

Existem diversas estratégias na literatura de mecanismos propostos para retardar a degradação do AH no organismo humano, destacando-se a reticulação química (ou *crosslinking*), associação com outras biomoléculas e associação com antioxidantes (FRASER et al., 1981; MATSUMURA; HERP; PIGMAN, 1966). Essas estratégias têm por objetivo aumentar o tempo de meia vida do AH no organismo, sem com que haja perda de propriedades interessantes como a biocompatibilidade. Dentre os grupos presentes na molécula de AH, os mais comumente utilizados como sítio de reticulação são o carboxil e o hidroxil (CAMPOCCIA et al., 1998; PRESTWICH, 2001).

3.1.6.1. Reticulação química com divinil sulfona (DVS).

A reticulação com a molécula de DVS acontece devido à formação de uma ligação éter no grupo hidroxil do AH (COLLINS; BIRKINSHAW, 2008). Para que essa reação ocorra, o meio reacional deve apresentar o pH alcalino (COLLINS; BIRKINSHAW, 2007). O meio alcalino induz a formação de radicais alcóxi e, em seguida, a geração de reticulações sulfonil-bis-etil entre grupos hidroxila e como consequência há a formação da matriz reticulada do hidrogel. (SHIMOJO et al., 2015). A reticulação química do DVS com AH é principalmente utilizada em protocolos ortopédicos. (BALAZS; LESHCHINER, 1984; RAMAMURTHI; VESELY, 2002; SANNINO et al., 2004). A Figura 6 mostra o esquema da reação entre DVS e AH.

Figura 6. Esquema da reação entre AH e DVS. Modificado de Shimojo et al. (2015).

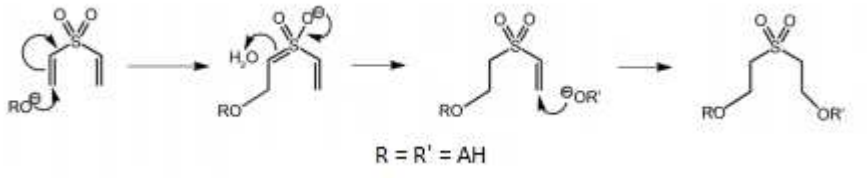

3.1.6.2. Reticulação com 4-Butanediol diglicidil éter (BDDE).

O BDDE é utilizado para estabilizar a maior parte do preenchedores dérmicos a base de AH presentes no mercado (TEZEL; FREDRICKSON, 2008). As moléculas de BDDE são biodegradáveis e possuem toxicidade significativamente reduzida se comparadas a outros agentes de *crosslink* baseados em ligações éter, como a DVS. A molécula de BDDE reage principalmente com os álcoois primários presentes nas cadeias do AH (ALLEMANN; BAUMANN, 2008; DE BOULLE et al., 2013). A Figura 7 apresenta uma molécula de AH reticulada com BDDE.

Figura 7. Representação de AH reticulado com BDDE. Modificado de Tezel e Fredrickson (2008).

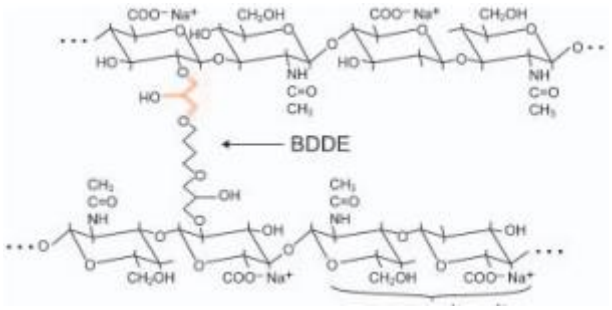

3.1.6.3. Oxidação parcial e reticulação com dihidrazida adípica (ADH).

Na presença de periodato de sódio ($NaIO_4$) o AH sofre oxidação parcial, o que promove a abertura do anel do ácido d-glucurônico e a formação de dois grupos aldeído, conforme pode ser observado na Figura 8.

Figura 8. Reação de oxidação de AH com periodato de sódio. Modificado de Lin et al. (2011).

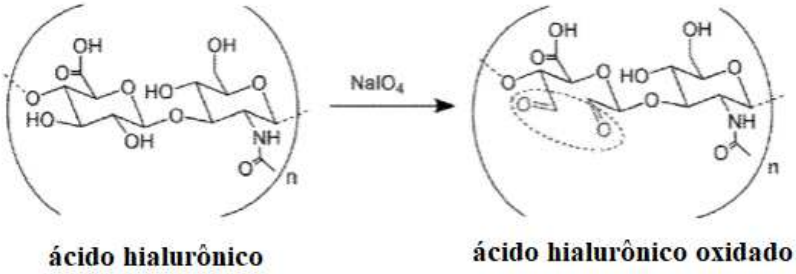

Essa reação química é lenta e de primeira ordem com relação ao periodato. Como consequência, a oxidação parcial das cadeias promove sua cisão, flexibilidade local e sua compactação, reduzindo sua viscosidade (KRISTIANSEN; DALHEIM; CHRISTENSEN, 2013; PAINTER; LARSEN, 1973). Há outros mecanismos de oxidação parcial do AH, como a oxidação por meio de 2,2,6,6-Tetramethyl-1-piperidinyloxy (tempo), o qual requer a utilização de pelo menos um agente co-oxidante, enquanto a oxidação com periodato tem a vantagem de apenas utiliza $NaIO_4$ (BUFFA et al., 2012).

Devido a sua fácil obtenção e propriedades, é possível encontrar estudos na literatura com diversas aplicações do oxi-AH. Crescenzi e Francescangeli (2003) reportaram que sais de oxi-AH/Zn possuem expressiva atividade antibacteriana contra bactérias S. aureus. Sheu e colaboradores (2013) desenvolveram um hidrogel a partir da associação de oxi-AH com resveratrol com a finalidade de regenerar danos causados pela osteoartrite na cartilagem. Os resultados obtidos pelo grupo de pesquisa foram positivos para a encapsulação de células, entretanto os pesquisadores apontam a necessidade de testes *in vivo* para que sejam possível futuras aplicações desse material. Li et al. (2014) desenvolveram um hidrogel de oxi-AH e quitosana com reticulação *in situ* com a intenção de evitar a adesão do peritônio no período pós-operatório. O peritônio é uma estrutura do corpo humano responsável por envolver órgãos viscerais e esse fenômeno pode causar diversas alterações importantes e danosos no organismo humano. Cai et al. (2017) desenvolveram um hidrogel de quitosana associado com oxi-AH para liberação controlada de oligonucleotidios e seus efeitos silenciador de genes (CAI et al., 2017).

A oxidação parcial do AH e o surgimento de grupos aldeído possibilita a reação *click* entre moléculas de oxi-AH e ADH, ou seja, uma reação de reticulação química que não necessita da presença de catalisadores ou de fontes externas de energia (LIN et al., 2012; MA et al., 2017). Reações químicas *click* se caracterizam por serem termodinamicamente

favoráveis, não produzirem subprodutos tóxicos e por possuírem altas taxas de rendimento. Para que uma reação seja caracterizada como *click* os reagentes devem estar prontamente disponíveis, deve ser evitado o uso de solventes, ou então devem ser utilizados solventes atóxicos e facilmente separáveis do meio reacional (KOLB; FINN; SHARPLESS, 2001). A Figura 9 apresenta a reação química da reticulação de oxi-AH com ADH.

Figura 9. Reação de reticulação de oxi-AH com ADH. Retirado de Lin et al. (2011).

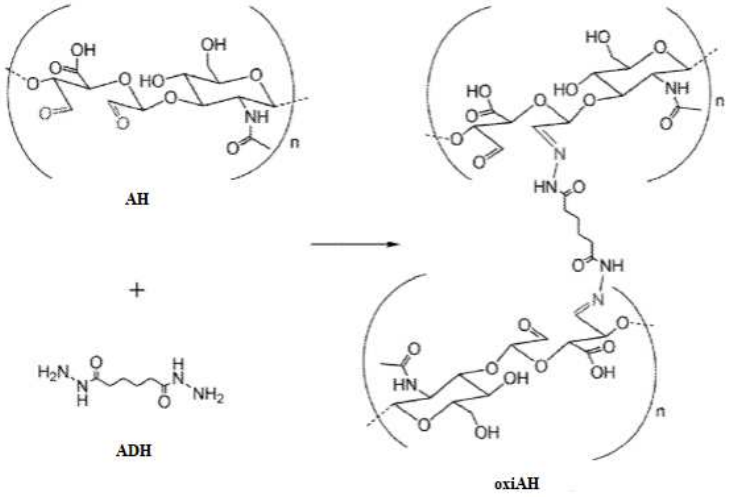

Na literatura é possível encontrar diversos trabalhos envolvendo a reticulação de oxi-AH com ADH. Jia et al. (2004) produziram o hidrogel de oxi-AH/ADH com a finalidade de estudar sua biocompatibilidade em um modelo animal de bloqueio do nervo ciático e obtiveram resultados positivos. Su, Chen e Li (2010) estudaram a possibilidade do hidrogel oxi-AH/ADH ser utilizado para a regeneração do núcleo pulposo, uma estrutura presente na coluna vertebral. Lin et al. (2011) patentearam um protocolo para utilização de oxi-AH/ADH hidrogéis para a substituição do humor vítreo. Shoham et al. (2013) produziram oxi-AH/ADH e estudaram seu potencial de entrega de células em tecido adiposo danificado. Mais recentemente, Weis et al. (2018) estudaram diferentes formulações de oxi-AH/ADH a fim de se utilizar esse material como biotinta em impressões 3-D.

3.2. Espécies reativas de oxigênio.

Todos os organismos aeróbicos estão sujeitos à ação de espécies reativas de oxigênio (ROS), um grupo de moléculas que abrange peróxido de hidrogênio, alguns superóxidos e alguns radicais livres. ROS são capazes de provocar importantes danos a estruturas celulares, iniciando reações em cadeia capazes de desnaturar proteínas, romper

membranas lipídicas, danificar o DNA e promover a morte celular (MUNNÉ-BOSCH; PINTÓ-MARIJUAN, 2017).

Atualmente o papel de ROS é amplamente estudado, sobretudo a fim de se entender sua atuação no envelhecimento de células mesenquimais e como sinalizador para diferenciação celular. Estudos do envelhecimento celular mostraram que é possível promover a multiplicação de células-tronco em condições hipóxicas, ou seja, quando há baixa concentração de oxigênio, de maneira que a capacidade de diferenciação celular não fosse comprometida. Além disso, os mesmos estudos indicaram que em meios em que há a presença de peróxido de hidrogênio exógeno ocorre a senescência prematura dessas células (LYUBLINSKAYA et al., 2015).

3.3. Tempol.

Moléculas antioxidantes podem ser definidas como qualquer molécula capaz de retardar, prevenir ou remover qualquer dano oxidante causado em alguma molécula de interesse. Essas moléculas podem ser sintetizadas ou ocorrer naturalmente, como é o caso do ácido ascórbico presente em frutos cítricos e o resveratrol, encontrado nas sementes de uva (BURTON; INGOLD, 2015).

Tratamentos com antioxidantes atualmente são estudados como estratégia para retardar doenças degenerativas, as quais podem ser intensificadas pela presença de *stress* oxidativo. Em algumas dessas doenças degenerativas a ação de antioxidante endógenos não é suficiente para evitar danos expressivos causados por radicais livres. Antioxidantes exógenos podem ser adquiridos com uma alimentação equilibrada, rica de frutas e verduras, entretanto, há discrepâncias entre resultados de pesquisas que estudam a ação dessas substâncias na presença de doenças degenerativas (FERNANDES et al., 2014).

Em estudos relacionados à atividade antioxidante, o tempol (4-hidroxi-2,2,6,6-tetrametil-piperidine-1-oxil) é uma molécula comumente utilizada, pois se trata de uma molécula estável que, ao entrar em contato com radicais livres, age como um antioxidante tanto na sua forma original quanto na sua forma reduzida, tempol-H (DOS SANTOS et al., 2009). A Figura 10 apresenta a molécula de tempol.

Figura 10. Representação da molécula de tempol. Retirado de Dos Santos et al. (2009).

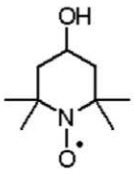

O tempol é um nitróxido sintético de baixa massa molar (172.24 Da), com alta permeabilidade celular, e estável na sua forma oxidada. Essa molécula é usualmente utilizada como substância padrão em análises de espectroscopia de ressonância paramagnética eletrônica (EPR) (DOS SANTOS et al., 2009; VALAVANIDIS et al., 2004).Trata-se de um antioxidante mais eficiente do que moléculas comumente utilizadas com esse propósito, como a n-acetilcisteína e algumas vitaminas. Além disso, o tempol é efetivo como catalase, prevenindo a formação de radical hidroxila e é considerado como agente *redox-recycling*, ou seja, se auto recicla nas reações de oxirredução, o que garante um tempo prolongado de ação (YEN; CHEN, 1995). A Figura 11 apresenta a representação do *redox-recycle* do tempol.

Figura 11. Auto reciclagem do tempol nas reações de oxidação e redução. Retirado de Wilcox & Pearlman (2008).

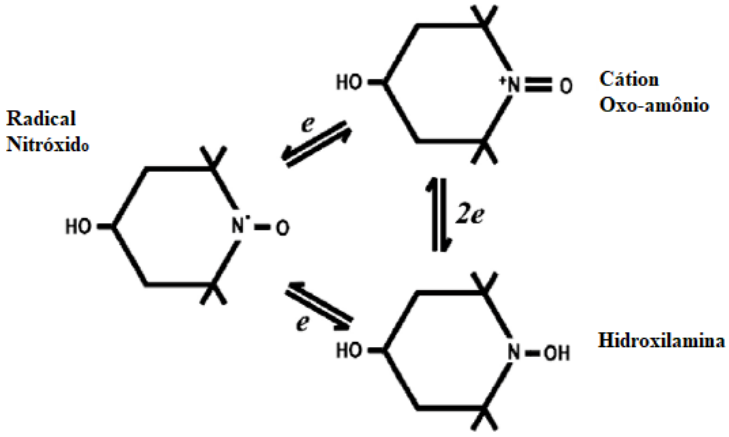

A utilização de tempol para aplicações médicas é segura considerando-se que se trata de uma molécula com baixa toxicidade. Sua dosagem tóxica é entre 1 e 2 mmol/kg, valor abaixo da dosagem efetiva (em torno de 10-4 mmol/L) em estudos de *stress* oxidante. Sua aplicação médica é interessante sobretudo por proteger células do *stress* oxidativo, mimetizando a ação da enzima superóxido desmutase (SOD). O tempol também apresenta a

capacidade de permear através de membranas celulares, o que a SOD não é capaz (CHATTERJEE et al., 2000; KRISHNA et al., 1992; SAMUNI et al., 1992; THIEMERMANN, 2003).

A Figura 12 apresenta as principais reações pró-oxidantes que ocorrem *in vivo* e as vias que induzem o dano oxidante das biomoléculas pelos radicais livres $O2^{\bullet-}$ e $NO^{\bullet}$. GSH representa glutationa reduzida, um tripeptídeo responsável pela proteção das células contra ação de radicais livres e GS-SG representa a glutationa oxidada.

Figura 12. Principais reações pro-oxidantes-antioxidante que ocorrem *in vivo* e as vias que induzem o dano oxidante das biomoléculas mediada pelos radicais livres $O_2^{\bullet-}$ e $NO^{\bullet}$. Modificado de Schnackenberg (2002).

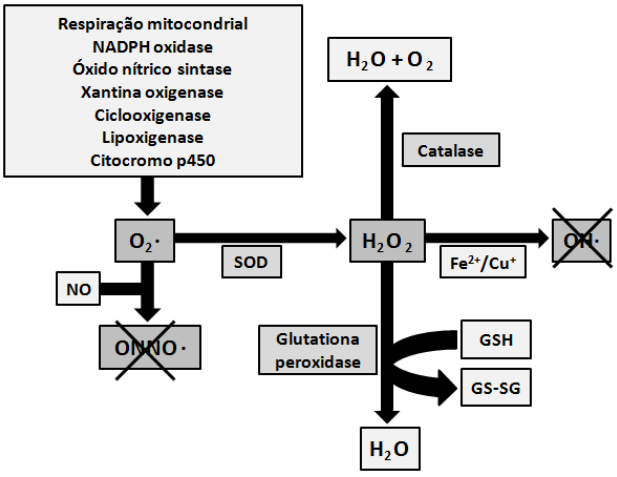

4. MATERIAL, MÉTODOS, RESULTADOS E DISCUSSÃO

Esta seção será apresentada na forma de capítulos referentes aos resultados desta pesquisa, sendo dois deles contendo artigos científicos.

O primeiro capítulo, constituído do artigo cujo título é *Partial periodate oxidation of hyaluronic acid: changes in the colloidal domain lead to improved properties for medical applications*. Esse artigo teve por objetivo caracterizar as mudanças no domínio coloidal causadas pela oxidação do AH e estudar sua influência na reticulação com ADH e na liberação sustentada do tempol.

O segundo capítulo, constituído do artigo cujo título é *Stability under oxidative stress of hydrogels of oxidized hyaluronic acid crosslinked with adipic dihydrazide and containing entrapped tempol,* teve por objetivo estudar a proteção oferecida pelo antioxidante tempol aos hidrogéis reticulados de oxi-AH/ADH nas configurações sólida e em micro e nanopartículas, submetidos ao stress oxidativo induzido por peróxido de hidrogênio.

4.1 Partial periodate oxidation of hyaluronic acid: changes in the colloidal domain lead to improved properties for medical applications.

Partial periodate oxidation of hyaluronic acid: changes in the colloidal domain lead to improved properties for medical applications

D.P. Sacomani[1], C.G. França[1], D. G. Villalva[1] and M. H. A. Santana[1].*

1Department of Engineering of Materials and Bioprocesses, School of Chemical Engineering, University of Campinas, 13083-852, Campinas, SP, Brazil.

*Correspondence should be addressed to mariahelena.santana@gmail.com

Declarations of interest: none

Abstract

Hyaluronic acid (HA) is a natural, biocompatible, biodegradable and water-soluble polysaccharide composed by the monomers D-glucuronic acid and N-acetyl-D-glucosamine. HA is the main component of human synovial fluid and abundant in the skin. Exogenous bio-HA has been used as a dermal filler and in orthopedic protocols mainly. However, the fast metabolism compromises its functions and the maintenance of its integrity *in vivo* is still a challenge. High molar mass HA as well as various types of chemical crosslinks has been applied as strategies to increase its half-life. The partial oxidation of HA provides changes in its colloidal domain which open novel possibilities for improved formulations. Here, we characterized the influence of the oxi-HA degree on the structural and interfacial changes of HA. In addition, we studied the oxi-HA modulation on chemical crosslinking with adipic dihydrazide (ADH) and modified release of the antioxidant tempol, a potent antioxidant with mimic action of superoxide dismutase in human tissues. The obtained results are relevant for designing novel HA formulations with improved injectability, *in situ* crosslinking and *in vivo* stability.

Keywords: oxidized hyaluronic acid, zeta potential, hydrodynamic diameter

1. Introduction

Hyaluronic acid (HA) is a natural polysaccharide found in most connective tissues and in synovial fluid. The primary HA structure is composed by the monomers D-glucuronic acid and N-acetyl-D-glucosamine linked together through alternating β-1,4 and β-1,3 glycosidic bonds arranged in large and linear chains (SHE; DINH; TU, 1974). When in solution, HA molecule occupies a large hydrated volume thanks to the presence of hydrophilic and hydrophobic domains that can lead to entanglements and viscoelastic properties (HASCALL; LAURENT, 1997). Therefore, physical crosslinking occurs in semi-diluted and concentrated regimes, stabilizing the HA structure (MALEKI; KJØNIKSEN; NYSTRÖM, 2008).

Due to its properties such as biocompatibility and similar structure to the extra cellular matrix, high molar HA is widely used in the medical field by itself or associated with other molecules. Some of those molecules are crosslinkers like divinyl sulfone which can be used in orthopedic protocols (BALAZS; LESHCHINER, 1984; RAMAMURTHI; VESELY, 2002; SANNINO et al., 2004), 1,4-Butanediol diglycidyl ether for dermal filler (ALLEMANN; BAUMANN, 2008; DE BOULLE et al., 2013) or chitosan in scaffolds, as strategies to increase its half-life (FANG et al., 2008; LIM et al., 2000; MAO et al., 2003; PARK et al., 2013).

It is well-known in the literature the various possibilities of chemical crosslinking of HA, which preserves its biocompatibility and makes it more resistant to chain degradation by metabolism and the presence of free radicals (FRASER et al., 1981; MATSUMURA; HERP; PIGMAN, 1966). The two most common groups used for crosslinking are the carboxyl and hydroxyl groups, and the main crosslinkers studied are biscarbodiimides, poly-functional epoxides and adipic acid dihydrazide (ADH) (CAMPOCCIA et al., 1998; PRESTWICH, 2001).

In the presence of sodium periodate, HA undergoes partial oxidation, leading to the opening of the D-glucuronic acid ring with the formation of two aldehyde groups, as shown in Figure 1 (LIN et al., 2012; MA et al., 2017). This chemical reaction is slow and is first order with respect to the periodate. Therefore, oxidation also promotes local flexibility and compaction of the chains, reducing HA viscosity (KRISTIANSEN; DALHEIM; CHRISTENSEN, 2013; PAINTER; LARSEN, 1973). More complex partial oxidation uses the radical TEMPO, requiring at least one co-oxidizing agent, whereas the periodate reaction only uses sodium periodate (BUFFA et al., 2012). The partial oxidation of HA also makes possible the click reaction between oxi-HA and ADH, a crosslinking strategy that does not involve the presence of catalysts and does not produce toxic byproducts (LIN et al., 2012; MA et al., 2017).

Figure 1. Partial oxidation of HA.

Due to its simplicity and properties, various applications of oxi-HA from partial periodate oxidation have been described in the scientific literature. Crescenzi and Francescangeli (2003) reported that oxi-HA/Zn salts have more substantial antibacterial activity against S. aureus bacteria than HA/Zn salts (CRESCENZI; FRANCESCANGELI, 2003). Su et al. (2010) produced an oxi-HA/ADH hydrogel for nucleus pulposus regeneration based on its biocompatibility and resistance to degradation (SU; CHEN; LIN, 2010). Cai et al. (2017) developed an oxi-HA/chitosan hydrogel for sustained release of gapmer antisense oligonucleotides and its effect on gene silencing and chondrocyte binding (CAI et al., 2017). Recently, Weis et al. (2018) studied the feasibility of oxi-HA/ADH as a bioink for 3D printing of ADH with different degrees of oxidation and concentrations, considering the biological advantage of HA to be a component of the extracellular matrix (WEIS et al., 2018).

Although the chemical crosslink can make exogenous HA more resistant to degradation, its association with antioxidants can be used as an extra protection against the effects of free radicals and treat diseases with a strong correlation with them (MITCHELL et al., 1990; SAMUNI et al., 1991; SCHUBERT et al., 2004). In the group of synthetic antioxidants, tempol (4-hydroxy-2,2,6,6-tetramethylpiperidin-1-oxyl) is a molecule that can be highlighted due its characteristics. Tempol is classified as a piperidine nitroxide, is water soluble and has low molar mass (MM) (172.24 Da) (DOS SANTOS et al., 2009). This antioxidant has also the ability to protect cells against oxidative stress and mimic the enzyme superoxide dismutase (SOD) since it can scavenge superoxide anions. Tempol also has the advantage of permeating through biological membranes, which SOD is no able to do (CHATTERJEE et al., 2000; KRISHNA et al., 1992; SAMUNI et al., 1992; THIEMERMANN, 2003). Figure 2 shows the representation of a tempol molecule.

Figure 2. Structure of a tempol molecule.

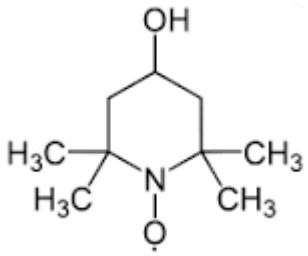

Although the colloidal domain of native and unmodified exogenous HA is well known, studies on oxi-HA behavior in the colloidal domain are limited. A better understanding of the molecular organization of structures can lead to the prediction and modification of its properties for specific applications. Besides that, there is a lack of studies in the literature that explore the possibilities of the association between HA and tempol. In the present work, we studied the influence of the oxi-HA oxidation degree on the structural and interfacial changes of HA was. In addition, we studied the oxi-HA modulation on chemical crosslinking with adipic dihydrazide (ADH) aiming *in situ* crosslinking, as well as its capability for entrapping and modified release of the antioxidant tempol, a potent antioxidant with mimic action of superoxide dismutase in human tissues, for improvement of its *in vivo* stability. The obtained results are relevant for the design of HA formulations with improved *in vivo* stability and injectability.

2. Materials and methods

2.1. Materials and reagents

HA, average MM of 9.48 x 10^5 Da, fractions of 10^4 Da (4.16 %), 10^5 Da (57.36 %) and 10^6 Da (38.48 %), was purchased from Shandong Topscience Biotech Co. (Rizhao City, Shandong Province, China). Sodium periodate ($NaIO_4$), ADH, ethylene glycol, trichloroacetic acid, picrysulfonic acid solution (TNBS), tert-butyl carbazate (t-BC) and tempol (4-hydroxy-2,2,6,6-tetramethylpiperidine-N-oxyl) were purchased from Sigma-Aldrich, Inc. (St. Louis, MO, USA). Dialysis membranes with a nominal MWCO of 12,000-16,000 Da were purchased from Inlab (Diadema, SP, Brazil).

2.2. Methods

2.2.1. Preparation of oxi-HA

Oxi-HA was synthesized according to the methods proposed by Lin et al. (2012) and Ma et al. (2017). HA (1 % w/v in Milli-Q water) was mixed with sodium periodate (10.67 % w/v) at room temperature under agitation for 24, 48 or 72 h in a beaker wrapped with

aluminum foil. The molar ratios of HA: $NaIO_4$ were 1:0.5, 1:1, 1:2, 1:3 and 1:4. The reaction was quenched by the addition of ethylene glycol (the proportion of ethylene glycol to $NaIO_4$ was 1:6) and stirred for 0.5 h. The resulting solution was dialyzed by a dialysis membrane (MWCO of 12,000-16,000 Da) for 3 days with water being changed at least twice daily. Finally, the dialyzed solution was lyophilized to yield a white fluffy product.

2.2.2. Preparation oxi-HA/ADH hydrogel associated with tempol

The oxi-HA/ADH hydrogel was produced according to the protocols proposed by Lin et al. (2012) and Ma et al. (2017) with modifications. Briefly, 300 µL of oxi-HA (8 % w/v, PBS) were mixed with 100 µL of a tempol solution (5 % w/v, PBS) and then the solution was mixed with 100 µL of ADH (8 % w/v, PBS). Then the hydrogels were stored for 12 h at 4 °C to obtain complete gelation.

2.2.3. Oxidation degree

The degree of oxidation of oxi-HA was determined by quantifying the number of dialdehyde groups using a TNBS assay (LIN et al., 2012). Briefly, 25 µL of t-BC (30 mM) in a 1 % aqueous trichloroacetic acid was added to of 25 µL of oxi-HA (0.6 %), and the mixture could react in an Eppendorf tube at room temperature for 24 h. t-BC can react with aldehydes forming a stable carbazone in a similar manner to hydrazone formation, which can be quantified with TNBS. After 24 h, 0.5 mL of aqueous TNBS solution (6 mM, 0.1 M borate buffer, pH 8) was transferred to an Eppendorf tube to react with the excess t-BC for 60 minutes at room temperature. Then, this solution was diluted with 0.5 N hydrochloric acid with a proportion of 1:40 (v/v). The absorbance of the solution was measured with a Genesys 6 spectrophotometer (Thermo Fisher Scientific, Massachusetts, USA) at a wavelength of 330 nm. A standard calibration curve from t-BC solutions (5-30 mM) was used to determine the amount of unreacted t-BC and to convert the result into dialdehyde content. All experiments were performed in triplicate.

2.2.4. pH

The pH of the oxi-HA solutions was measured by an DM-22 pH meter (Digimed, São Paulo, Brazil). Oxi-HA was dissolved in Milli-Q water in a 0.1 % w/v concentration and the measures were done at room temperature.

2.2.5. Fourier transform infrared spectroscopy

The functional groups of oxi-HA with different degrees of oxidation were identified by Fourier transform infrared (FTIR) spectroscopy using a Nicolet 6700 instrument (Thermo

Scientific, Madison, USA) equipped with an attenuated total reflectance (ATR) accessory and a ZnSe crystal. The spectra were obtained in the range of 800-1800 cm-1, with a 4 cm-1 resolution and 128 scans.

2.2.6. Average hydrodynamic diameter

The average hydrodynamic diameter and the particle size distribution were determined by dynamic light scattering with a Zetasizer Nano ZS instrument (Malvern Panalytical, United Kingdom) using a Ne-He laser and measurements at a scattering angle of 90°. The hydrodynamic diameter was determined by the Stokes-Eintein equation (Equation 1).

$$Rh = k \times T/6 \times D \times \eta \qquad (1)$$

Where Rh é the hydrodynamic radius, k is the Boltzmann constant, T is the absolut temperature, D is the diffusion coefficient and η is the viscosity of the solvent.

The samples of HA and oxi-HA used in this analysis were diluted to a concentration of 0.1 % (w/v), and the measurements were done in triplicate. The mean hydrodynamic diameter, Z-average, were calculated according to Equation 2, the size distribution expressed as Intensity of scattering and Number of particles I-distribution ($I \alpha d^6$) and N-distribution ($I \alpha d$) respectively, and the polydispersity by the polydispersity index (PDI).

$$\text{Z-average} = \sum(n_i \times d_i^3)/ \sum(n_i \times d_i^2) \qquad (2)$$

Where n_i is the number of particles with a diameter, d_i.

2.2.7. Zeta potential

The zeta potential was measured in a Zetasizer Nano ZS. Solutions at a concentration of 0.1 % (w/v) at 25ºC and an optical path of 1 cm were used. The refractive and absorbance indices used for oxi-HA were 1.33 and 0.001 AU, respectively. The measurements were acquired in triplicate.

2.2.8. Viscosity

An SV-10 viscometer (A&D Company, Ltd, Tokyo, Japan) was used to determine the viscosity of HA and oxi-HA solutions. The temperature of the solutions was also measured, and the concentration used was 1 % (w/v).

2.2.9. Swelling of hydrogels

The swelling properties of the hydrogels was determined by submerging each sample in PBS for 24 h and then lyophilizing them. The swelling was calculated by weighting each sample before and after lyophilization. The swelling was calculated according to the Equation 3:

$$\text{Swelling } (\%) = 100 \times (wp - wd)/wd \qquad (3)$$

Where wp is the mass of each hydrogel after 24 h in PBS wd is the mass of each sample after lyophilization.

2.2.10. Scanning electron microscopy

The Scanning electron microscopy (SEM) was used to study the structure of the hydrogels. The metal coating was made with a Sputter Coater POLARON, model SC7620 (VG Microtech, Uckfield, England). The micrographs were obtained using a Scanning electron microscope model Leo 440i with energy dispersive x-ray detector model 6070 (LEO Electron Microscopy/Oxford, Cambridge, England), with 50 pA and 10 kV.

2.2.11. Release of tempol

Tempol's release curve by the hydrogel was constructed by measuring tempol's concentrations in PBS by a Thermo Electron Spectronic GENESYS 6 UV-Visible Spectrophotometer (Waltham, Massachusetts, United States) during time intervals. The hydrogels produced in the presence of tempol were submerged in PBS inside an Eppendorf which had its lid removed. A dialysis membrane (MWCO of 12,000-16,000 Da) was used to cover the Eppendorf's open end and the Eppendorf was put inside a falcon tube which had PBS in so that the membrane was slightly submerged in the PBS. The PBS concentration outside of the Eppendorf was the one that was measured during the assay. A previously constructed analytical curve with tempol concentrations ranging between 0.3 to 2 mg/mL at 428 nm was used.

3. Results and discussion

3.1 Characterization of oxi-HA

Table 1 summarizes the theoretical degrees of oxidation calculated from the molar ratio of $NaIO_4$ and HA (LIN et al., 2012) and the results obtained by the TNBS assay.

Table 1. Oxidation degrees of oxi-HA.

Molar ratio HA:$NaIO_4$	**Reaction time (h)**	**Theorical oxidation degree (%) ***	**Experimental oxidation degree (%)**
1:0.5	24	50	26 ± 6
1:1		100	44 ± 4
1:2			65 ± 5
1:3			82 ± 5
1:4			88 ± 7
1:0.5	48	50	24 ± 4
1:1		100	26 ± 6
1:2			66 ± 5
1:0.5	72	50	37 ± 6
1:1			83 ± 4
1:2			90 ± 11

*The theoretical oxidation degree was calculated according to Lin et al. (2012) [21].

It can be observed that the theoretical degree of oxidation was not reached in any of the samples. As expected, the degree of oxi-HA increased with increasing $NaIO_4$ for the reaction time of 24 h, except for the 1:4 ratio of HA:$NaIO_4$ due to diffusional limitations. For the same HA: $NaIO_4$ ratios, the degree of oxidation did not increase significantly from 24 hours, but from 24 h to 72 h it increased. Therefore, for further experiments, the 1:1, 1:2 and 1:3 HA:$NaIO_4$ ratios and a 24 h reaction time were chosen as the experimental conditions and named oxi-HA1, oxi-HA2 and oxi-HA3, respectively.

Figure 3 shows the obtained FTIR spectra of the samples of non-oxidized HA (A), oxi-HA1 (B), oxi-HA2 (C) and oxi-HA3 (D). These results were used to confirm the appearance of dialdehyde groups from the oxidation reaction (LIN et al., 2012). A new peak of aldehyde functional groups was observed in the FTIR spectra in C and D at 1717 and 1723 cm^{-1}, respectively, and in B, C and D at approximately 840 cm^{-1}, which is associated with the C=O stretching vibration of oxi-HA. The intensity of the peaks increased with the oxidation degree (from B to D). The peaks at 1152 and 893 cm^{-1} in spectrum A of non-oxidized HA were related to C-O-C (ether bond) and C-H as a control. The oxidation shifted to approximately 1116 cm^{-1}

and 874 cm^{-1} in spectra B, C and D because of the formation of aldehyde functional groups. These results are in accordance with those obtained by Lin et al. (2012) (LIN et al., 2012).

Figure 3. FTIR Spectra of (A) HA powder, (B) oxi-HA1, (C) oxi-HA2, and (D) oxi-HA3.

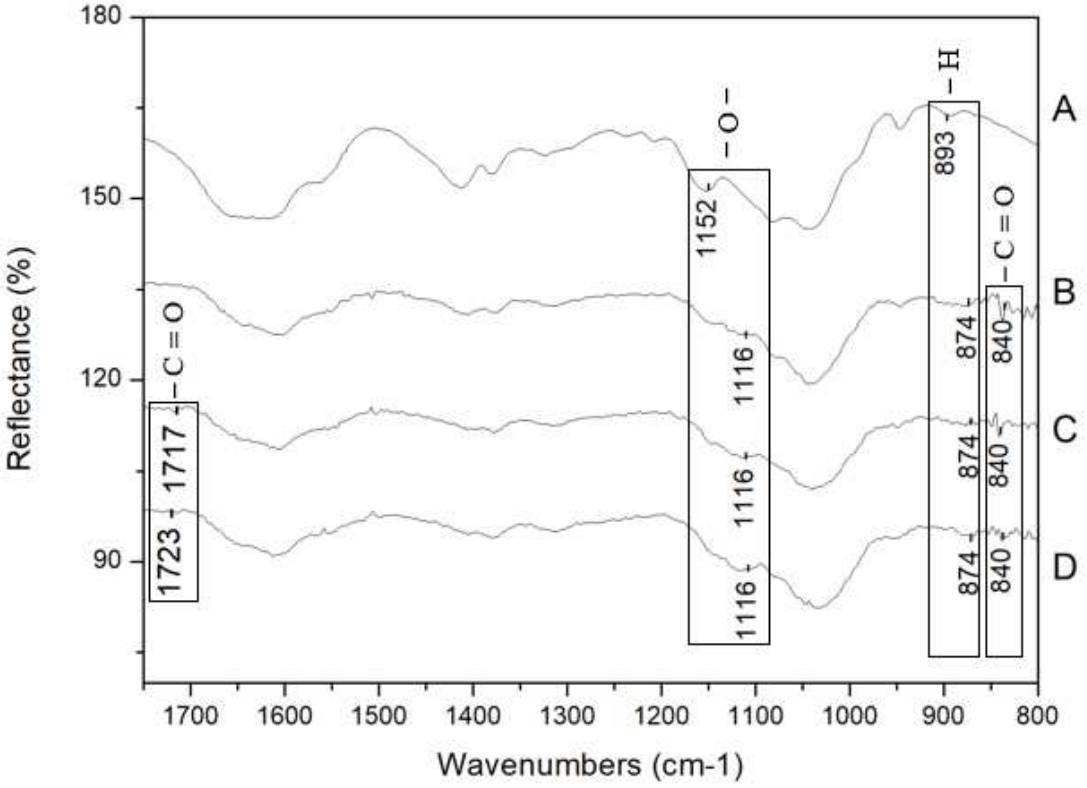

3.2. Changes in the colloidal domain

3.2.1. Size and distribution

Figure 4 shows the DLS spectra for the non-oxidized HA in terms of the intensity distribution (I), I α d^6, and number distribution (N), N α d. The results in the I distribution (Figure 4a) show three populations corresponding to the different HA globule densities provided by the MM distribution (10^4, 10^5 and 10^6 Da). The N distribution (Figure 4b) shows the prevalence of a less dense population in terms of particle number.

Figure 4. Size distributions of non-oxidized HA, oxi-HA1, oxi-HA2 and oxi-HA3, (a, c, e, g) intensity, (b, d, f, h) number.

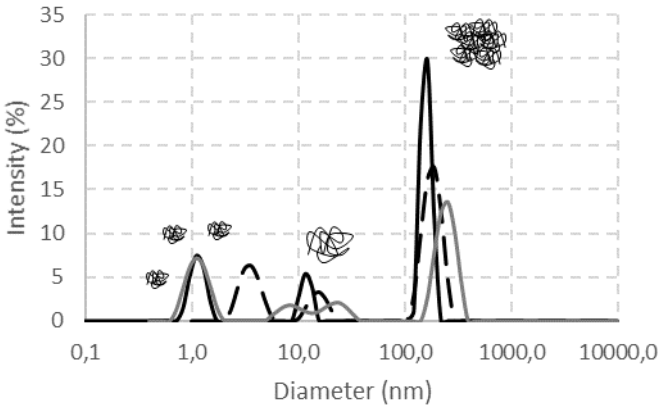

(a)

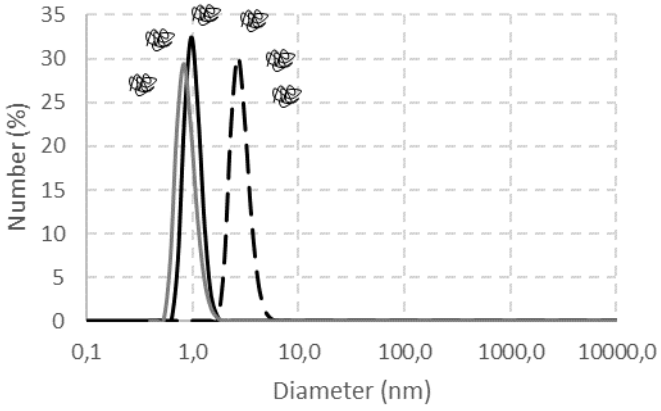

(b)

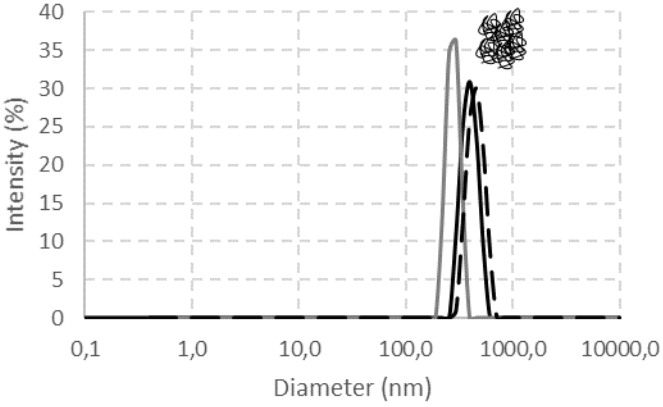

(c)

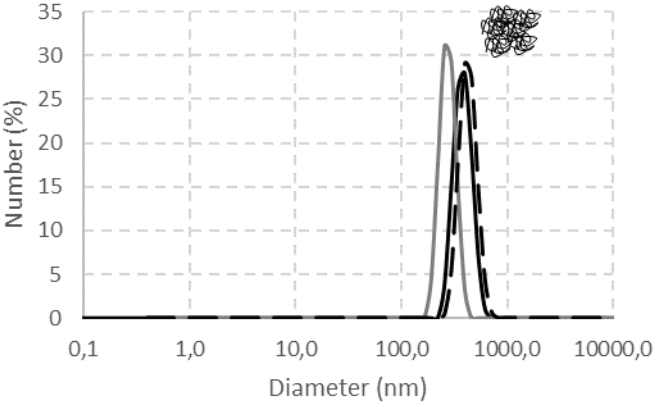

(d)

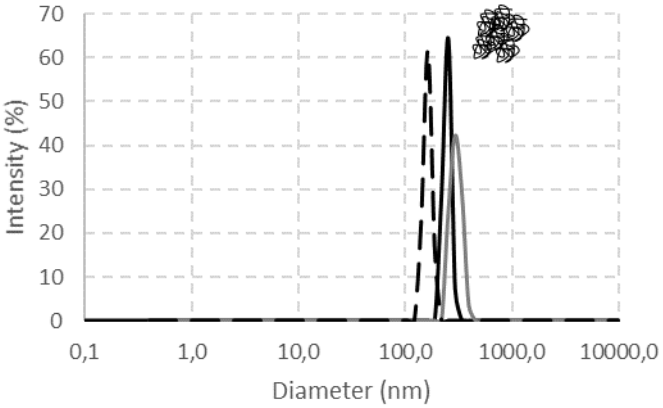

(e)

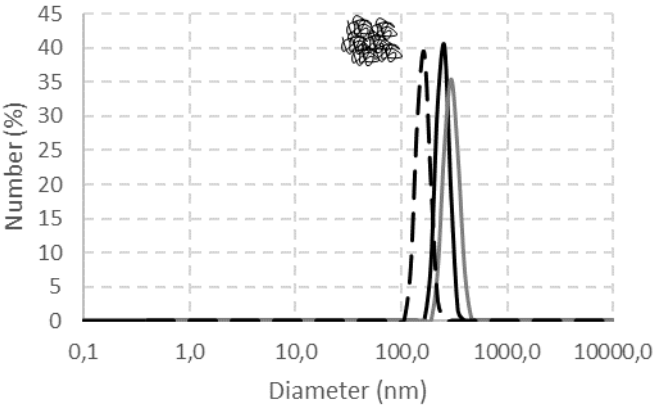

(f)

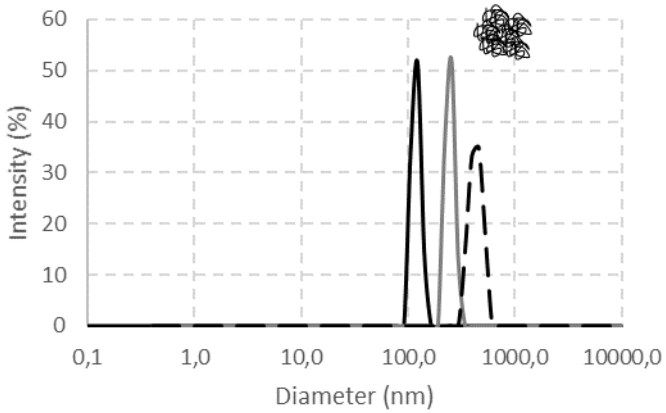

(g)

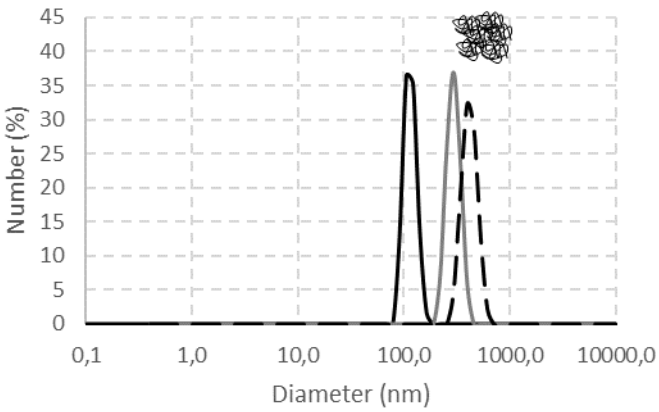

(h)

The oxidation of polysaccharides leads to local flexibility and compaction of the chains because of the opening of the D-glucuronic ring by sodium periodate, as proposed by Kristiansen et al. (2013). Therefore, denser structures with diameters in the range of 100-1000 nm were formed, as observed in the spectra of Figures 4c and 4d.

The increasing degree of oxidation led to a greater compaction of the structures, resulting in a slight displacement of the peaks to smaller diameters (approximately 100 nm), as observed in Figures 4e, f, g and h.

The corresponding values of the mean diameter and polydispersity of non-oxidized HA and oxi-HAs are shown in Table 2. As expected, the compaction of the structures provided by the oxidation degree reduced the Z-average and PDI. It can be observed also that the partial oxidation of the molecules influenced the pH of the oxi-HA solutions in Milli-Q water. There is a trend towards more basic solutions as there is na increase in the oxidation degree.

Table 2. Z-average and PDI of HA and oxi-HA.

Sample	**Degree of oxidation (%)**	**pH**	**Z-average (d·nm)**	**PDI**	**Zeta potential (mV)**	**Viscosity (mPa.s)**
HA	-	6.9 ± 0.2	1449 ± 193	0.99 ± 0.01	- 34 ± 13	391 ± 3
oxi-HA1	44 ± 4	7.6 ± 0.2	828 ± 108	0.6 ± 0.3	- 22 ± 7	1.64 ± 0.07
oxi-HA2	65 ± 5	8.1 ± 0.1	1011 ± 409	0.7 ± 0.2	- 46 ± 5	1.47 ± 0.05
oxi-HA3	82 ± 5	8.1 ± 0.2	1052 ± 329	0.7 ± 0.1	- 43 ± 5	1.26 ± 0.08

3.2.2. Zeta potential and viscosity

The entangled structure of non-oxidized HA presented a negative zeta potential (-34 ± 13 mV) due to the internal and external distribution of its dissociated carboxyl groups. The low oxidation degree in oxi-HA1 produced mixed structures of compacted and non-compacted HA, which changed the zeta potential to -22 ± 7 mV. The major structural changes were observed in oxi-HA2 and oxi-HA3. The flexibility of the chains caused by the opening of the D-glucuronic ring associated with the compaction of the non-oxidized N-acetyl amine portions exposed the negative charge of the dissociated carboxyl groups to the surface of the structure, resulting in a more negative zeta potential (-46 ± 5 and -43 ± 5 mV for oxi-HA2 and oxi-HA3, respectively). These changes are also reflected in the viscosity reduction in the oxi-HAs, due to the alignment of the chains allowing fast fluid flow, compared to the overlapping and stiff domains from the physical crosslinks in non-oxidized HA. The decrease in viscosity improve injectability in oxi-HA formulations.

Figure 5 shows a schematic depicting illustrating the changes in the colloidal domain of HA due to partial oxidations, that lead to alignment of the chains and compaction of the structures due to the opening of D-glucuronic acid ring.

Figure 5. Scheme of the local flexibility of the HA (A) chains and compaction of the structures caused by the opening of the D-glucuronic acid ring (B).

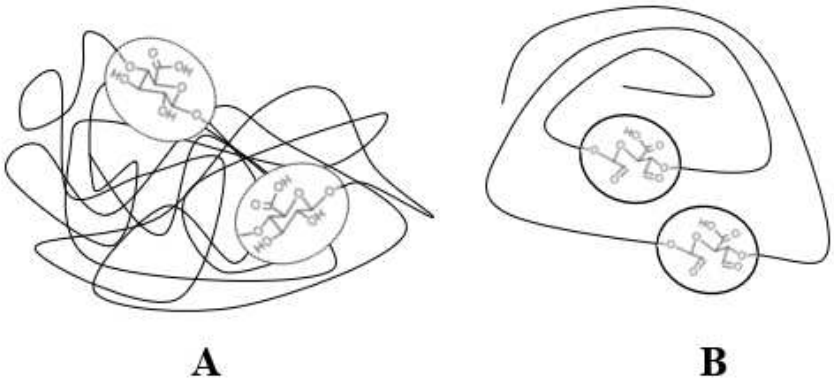

3.3. Modulation of oxi-HA/ADH hydrogels

3.3.1. Swelling capacity

The partial oxidation of HA makes possible the crosslinking with ADH without the necessity of catalysts or external sources of energy. The properties of the hydrogel can be

modulated varying the oxidation. Table 3 presents the swelling of each hydrogel. Although the hydrogels produced with oxi-HA2 and oxi-HA3 have similar swelling values, the hydrogel oxi-HA1 had a significantly higher swelling, which indicates lower crosslinking degree. These variations in the swelling are connected to the crosslinking degree and these results suggest the possibility of modulation of the hydrogels properties by varying the degree of oxidation of oxi-HA.

Table 3. Swelling of hydrogels.

Sample	Swelling (%)
oxi-HA1/ADH	94.9 ± 0.8
oxi-HA2/ADH	90 ± 1
oxi-HA3/ADH	91.20 ± 0.09

3.3.2. SEM micrographs

Figure 6 shows the micrographs obtained by SEM of the hydrogels. The microscopies show the material morphology, whose structure has a high concentration of pores and cavities evenly distributed. From these images, it can be observed that the oxi-HA oxidation degree can modulate the size and distribution of pores, since Figure 6a appears to have a higher number of cavities, while Figures 6b and 6c seem to have fewer negative spaces, which correlates to the swelling analysis. Although the hydrated material may not have the same pores dimensions, the micrographs show the path that tempol molecules go through during its diffusion from the hydrogel to the PBS solution.

Figure 6. SEM micrographs obtained for hydrogels with oxi-HA1 (a), oxi-HA2 (b) and oxi-HA3 (c) hydrogels.

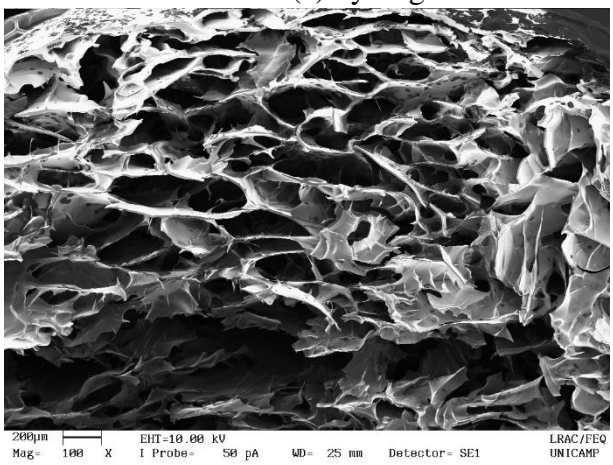

(a) Oxi-HA1/ADH

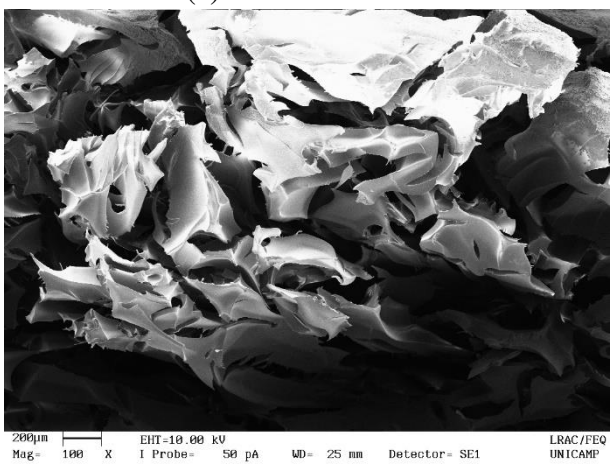

(b) Oxi-HA2/ADH

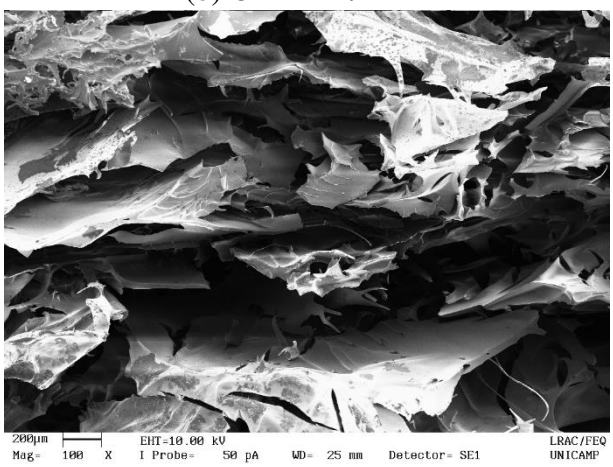

(c) Oxi-HA3/ADH

3.3.3. Sustained release of tempol by the hydrogels

Three types of oxi-HA/ADH hydrogels were produced using a fixed concentration of ADH (8 % w/v) and varying the degree of oxidation of oxi-HA (oxi-HA1, oxi-HA2 and oxi-

HA3). Figure 7 shows the concentrations of tempol in PBS during time intervals for 6 hours. It can be observed that the concentration equilibrium was reached after approximately 3 hours for the three types of hydrogels used, regardless of the degree of oxidation of oxi-HA. Although there are some differences in the tempol release rates between the types of hydrogels. The fact that the equilibrium was reached under 5 h can be explained by tempol's low MM. The molecules' small size and the fact that they are not chemically bonded with the crosslinked matrix allow them to easily diffuse from hydrogel to the PBS. It is expected that the hydrogels could have retained part of tempol's molecules due to the presence of -OH groups both in the antioxidant and in the HA's molecule, which leads to the formation of hydrogen bonds.

Figure 7. Sustained release of tempol.

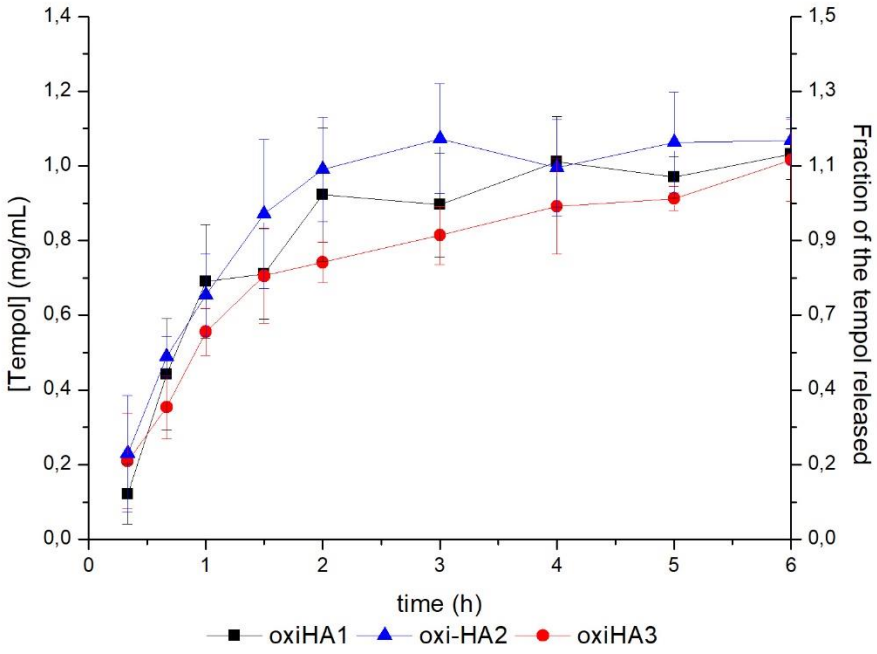

4. Conclusions

The results presented in this study show that HA was successfully oxidized in the presence of sodium periodate with various degrees of oxidation. The sodium periodate concentration had a greater effect on the degree of oxidation compared to the same reaction time. Partial oxidation caused important structural changes, as evidenced by the variations in mean diameter, size distribution, zeta potential and viscosity of the dispersions. These changes resulted from greater flexibility and alignment of the chains as well as the compaction of the

oxidized structures that allowed click crosslinking reaction with ADH. Tempol was totally incorporated in the oxi-HA/ADH during gelation and released in 6h. These results open perspectives to HA formulations with improved injectability, *in situ* gelation and stability under oxidative stress, which are useful for medical applications.

Author contributions

All authors contributed to the conception and design of this study and to the acquisition and analysis of the data. All authors contributed to the drafting and revising of this article and have approved the final version to be submitted.

Acknowledgments

This work was supported by the National Council for Scientific and Technological Development (process 10924/2017-5 and 153611/2016-2).

5. References

ALLEMANN, I. B.; BAUMANN, L. Hyaluronic acid gel (JuvédermTM) preparations in the treatment of facial wrinkles and folds. **Clinical Interventions in Aging**, v. 3, n. 4, p. 629–634, 2008.

BALAZS, E. A.; LESHCHINER, A. **Cross-Linked Gels of Hiyaluronic Acid and Products Containing Such Gels**, 1984.

BUFFA, R. et al. **METHOD OF PREPARATION OF AN OXIDIZED DERIVATIVE OF HYALURONIC ACID AND A METHOD OF MODIFICATION THEREOF**. United States, 2012.

CAI, Y. et al. A hyaluronic acid-based hydrogel enabling CD44-mediated chondrocyte binding and gapmer oligonucleotide release for modulation of gene expression in osteoarthritis. **Journal of Controlled Release**, v. 253, p. 153–159, 2017.

CAMPOCCIA, D. et al. Semisynthetic resorbable materials from hyaluronan esterification. **Biomaterials**, v. 19, p. 2101–2127, 1998.

CHATTERJEE, P. K. et al. Tempol, a membrane-permeable radical scavenger , reduces oxidant stress-mediated renal dysfunction and injury in the rat. **Kidney International**, v. 58, p. 658–673, 2000.

CRESCENZI, V.; FRANCESCANGELI, A. Note: Biological activity of C6-oxidized hyaluronic acid: Antibacterial properties of the Zn(II) salt. **Journal of Bioactive and Compatible Polymers**, v. 18, n. 3, p. 229–235, 2003.

DE BOULLE, K. et al. A review of the metabolism of 1,4-butanediol diglycidyl ether-crosslinked hyaluronic acid dermal fillers. **Dermatologic Surgery**, v. 39, n. 12, p. 1758–1766, 2013.

DOS SANTOS, A. B. et al. Antioxidant properties of plant extracts: An EPR and DFT comparative study of the reaction with DPPH, TEMPOL and spin trap DMPO. **Journal of the Brazilian Chemical Society**, v. 20, n. 8, p. 1483–1492, 2009.

FANG, J. Y. et al. Temperature-sensitive hydrogels composed of chitosan and hyaluronic acid as injectable carriers for drug delivery. **European Journal of Pharmaceutics and Biopharmaceutics**, v. 68, n. 3, p. 626–636, 2008.

FRASER, J. R. F. et al. Plasma clearance, tissue distribution and metabolism of hyaluronic acid injected intravenously in the rabbit. **Biochemical Journal**, v. 200, n. 2, p. 415–424, 1981.

HASCALL, V. C.; LAURENT, T. . **Hyaluronan: structure and physical properties**. Disponível em: <http://glycoforum.gr.jp/science/hyaluronan/HA01/HA01E.html>. Acesso em: 9 out. 2017.

KRISHNA, M. C. et al. Oxoammonium cation intermediate in the nitroxide-catalyzed dismutation of superoxide. **Proceedings of the National Academy of Sciences**, v. 89, n. 12, p. 5537–5541, 1992.

KRISTIANSEN, K. A.; DALHEIM, M. Ø.; CHRISTENSEN, B. E. Periodate oxidation and macromolecular compaction of hyaluronan. **Pure and Applied Chemistry**, v. 85, n. 9, p. 1893–1900, 2013.

LIM, S. T. T. et al. Preparation and evaluation of the *in vitro* drug release properties and mucoadhesion of novel microspheres of hyaluronic acid and chitosan. **Journal of controlled release : official journal of the Controlled Release Society**, v. 66, n. 2–3, p. 281–292, 2000.

LIN, F.-H. et al. **CROSS-LINKED OXIDATED HYALURONIC ACID FOR USE ASA VITREOUS SUBSTITUTE.** United States, 2012.

MA, X. et al. Improvement of toughness for the hyaluronic acid and adipic acid dihydrazide hydrogel by PEG. **Fibers and Polymers**, v. 18, n. 5, p. 817–824, 2017.

MALEKI, A.; KJØNIKSEN, A. L.; NYSTRÖM, B. Effect of pH on the behavior of hyaluronic acid in dilute and semidilute aqueous solutions. **Macromolecular Symposia**, v. 274, n. 1, p. 131–140, 2008.

MAO, J. S. et al. The properties of chitosan-gelatin membranes and scaffolds modified with hyaluronic acid by different methods. **Biomaterials**, v. 24, n. 9, p. 1621–1629, 2003.

MATSUMURA, G.; HERP, A.; PIGMAN, W. Depolymerization of Hyaluronic Acid by Autoxidants and Radiations. **Radiation Research**, v. 28, n. 4, p. 735–752, 1966.

MITCHELL, J. B. et al. Biologically Active Metal-Independent Superoxide Dismutase Mimics. **Biochemistry**, v. 29, n. 11, p. 2802–2807, 1990.

PAINTER, T.; LARSEN, B. A further illustration of nearest-neighbour auto-inhibitory effects in the oxidation of alginate by periodate ion. **Acta Chemica Scandinavica**, v. 27, p. 1957–1962, 1973.

PARK, H. et al. Injectable chitosan hyaluronic acid hydrogels for cartilage tissue engineering. **Acta Biomaterialia**, v. 9, n. 1, p. 4779–4786, 2013.

PRESTWICH, G. D. **Biomaterials from chemical-modified hyaluronan**. Disponível em: <http://glycoforum.gr.jp/science/hyaluronan/HA18/%0AHA18E.html>.

RAMAMURTHI, A.; VESELY, I. Smooth muscle cell adhesion on crosslinked hyaluronan gels. **J Biomed Mater Res**, v. 60, n. 1, p. 195–205, 2002.

SAMUNI, A. et al. Nitroxide stable radicals protect beating cardiomyocytes against oxidative damage. **Journal of Clinical Investigation**, v. 87, n. 5, p. 1526–1530, 1991.

SAMUNI, A. et al. Tempol, a Stable Free Radical, Is a Novel Murine Radiation Protector. **Cancer Research**, v. 52, n. 7, p. 1750–1753, 1992.

SANNINO, A. et al. Cellulose derivative-hyaluronic acid-based microporous hydrogels cross-linked through divinyl sulfone (DVS) to modulate equilibrium sorption capacity and network stability. **Biomacromolecules**, v. 5, n. 1, p. 92–96, 2004.

SCHUBERT, R. et al. Cancer chemoprevention by the antioxidant tempol in Atm-deficient mice. **Human Molecular Genetics**, v. 13, n. 16, p. 1793–1802, 2004. SHE, C. Y.; DINH, N. D.; TU, A. T. Laser raman scattering of glucosamine, n-acetylglucosamine, and glucuronic acid. **Biochimica et Biophysica Acta**, v. 372, p. 345–357, 1974.

SU, W. Y.; CHEN, Y. C.; LIN, F. H. Injectable oxidized hyaluronic acid/adipic acid dihydrazide hydrogel for nucleus pulposus regeneration. **Acta Biomaterialia**, v. 6, n. 8, p. 3044–3055, 2010.

THIEMERMANN, C. Membrane-permeable radical scavengers (tempol) for shock, ischemia-reperfusion injury, and inflammation. **Crit Care Med.**, v. 31, n. 0090-3493, p. S76–S84, 2003.

WEIS, M. et al. Evaluation of Hydrogels Based on Oxidized Hyaluronic Acid for Bioprinting. **Gels**, v. 4, n. 4, p. 82, 2018.

4.2 Stability under oxidative stress of hydrogels of oxidized hyaluronic acid crosslinked with adipic dihydrazide and containing entrapped tempol.

Stability under oxidative stress of hydrogels of oxidized hyaluronic acid crosslinked with adipic dihydrazide and containing entrapped tempol

D.P. Sacomani,1, C.G. França1 and M. H. A. Santana1*.
*Correspondence should be addressed to mariahelena.santana@gmail.com
1Department of Engineering of Materials and Bioprocesses, School of Chemical Engineering, University of Campinas, 13083-852, Campinas, SP, Brazil.

Declarations of interest: none

Abstract

The antinociceptive and anti-inflammatory actions of intra-articular injections of exogenous hyaluronic acid (HA) have been recognized as a modifier of the osteoarthritic state. However, the low half-life of HA *in vivo* still is a limiting factor for medical therapies. The oxidative stress caused by the reactive species of oxygen (ROS) is one of the main factors that compromise stability even for HA of high molar mass. This work aimed to study the stability under oxidative stress of hydrogels of oxidized hyaluronic acid (oxi-AH) crosslinked with adipic dihydrazide (ADH) and containing entrapped tempol. The hydrogels were configurated in solid matrices or in nano and microparticles. Tempol is a low molar mass (172.24 Da) synthetic antioxidant classified as a piperidine nitroxide that can undergo redox-recycling reactions and mimic the enzyme superoxide dismutase (SOD) in the biological medium. The oxidative stress was induced by hydrogen peroxide, and degradation of the matrices was determined along the time. The results showed that the presence of tempol increased the stability of the oxi-HA/ADH hydrogels, which was modulated by ADH crosslinking. The presence of nano or microparticles increased the stability of the matrices secondly. The stability under the oxidative stress reached 23 days for the more oxidized and crosslinked solid matrix containing tempol and added micro or nanoparticles in its formulation. These results are relevant for the development of long-lasting HA formulations for tissue engineering and treatment of orthopedic diseases.

Keywords: hyaluronic acid, tempol, oxidative stress

1. Introduction

Hyaluronic acid (HA) is a glycosaminoglycan composed by d-glucuronic acid and n-acetylglucosamine units which are linked by β-1,3 and β-1,4 glycosidic bonds and arranged in large linear chains (GARG; HALES, 2004; SHE; DINH; TU, 1974). HA can be found in throughout the human body in different concentrations and molar mass (MM). In the synovial fluid HA concentration ranges from 2 to 4 g/L and its MM is 6 -7 x 106 Da (GARG; HALES, 2004).

2. Materials and methods

2.1. Materials and reagents

HA with average MM of 9.48 x 10^5 Da was purchased from Shandong Topscience Biotech Co. (Rizhao City, Shandong Province, China). Sodium periodate ($NaIO_4$), ethylene glycol, tempol (4-hydroxy-2,2,6,6-tetramethylpiperidine-N-oxyl), ADH, trichloroacetic acid, picrysulfonic acid solution (TNBS), tert-butyl carbazate (t-BC), phosphate buffer solution (PBS), ABTS (2,2′-Azino-bis(3-ethylbenzthiazoline-6-sulfonic acid)), DPPH (2,2-Diphenyl-1-picrylhydrazyl), potassium persulfate ($K_2S_2O_8$), hydrogen peroxide solution (H_2O_2) were purchased from Sigma-Aldrich, Inc. (St. Louis, Missouri, USA). Dialysis membranes with a nominal MWCO of 12,000-16,000 Da were purchased from Inlab (Diadema, São Paulo, Brazil).

Intra-articular injections of exogenous HA have been recognized as a modifier of the osteoarthritic state, with antinociceptive and anti-inflammatory actions beyond boundary lubrication and shock absorption (BALAZS; DENLINGER, 1993; BROCKMEIER; SHAFFER, 2006; WATTERSON; ESDAILE, 2000). Particularly in osteoarthritis, the inflammatory cytokine IL-1β increases nitric oxide (NO) synthesis and decreases expression of the antioxidant enzymes that scavenge ROS, including superoxide dismutase, catalase, and glutathione peroxidase thereby accelerating the deleterious effects of oxygen radicals on cartilage. ROS induce cleavage of HA chains, and the oxidative stress is one of the leading causes of the short half-life of non-modified exogenous HA (less than 1 day).

Chemical crosslinks have emerged as strategies for increasing the half-life of HA, and various commercial with half-life times ranging from 1 day to 4 weeks have brought clinical benefits. However, difficulties in the injectability of highly crosslinked products, as well as adverse effects of some types of crosslinkers, have led to the search for complementary

strategies such as the derivatization of HA with antioxidants such as resveratrol (SHEU et al., 2013).

Tempol is a low molar mass (172.24 Da) synthetic antioxidant classified as a piperidine nitroxide (DOS SANTOS et al., 2009). It is a spin marker used as a standard in electron paramagnetic resonance (EPR) spectroscopy and in assays to measure antioxidant activity of compounds (DOS SANTOS et al., 2009; VALAVANIDIS et al., 2004; YEN; CHEN, 1995). Tempol can undergo redox-recycling reactions and mimic of the enzyme superoxide dismutase (SOD), and in the biological medium, it protects cells against oxidative stress by scavenging superoxide anions. Compared with SOD, tempol has the advantage of permeating through biological membranes (DOS SANTOS et al., 2009; YEN; CHEN, 1995).

Other known biological actions of tempol are the protection of blood proteins and lipids against peroxynitrite-mediated oxidative damage (VALAVANIDIS et al., 2004) and the inhibition of neutrophil and DNA damage mediated by hydrogen peroxide (DOS SANTOS et al., 2009; VALAVANIDIS et al., 2004). Therefore, the association of tempol to HA represents a valuable strategy for increasing its half-life in vivo. Except by derivatization, the entrapment of tempol in non-modified HA matrices is limited by its small size.

Dodero et al. (2018) studied the physical entanglement of high MM HA chains and calculated its matrix mesh size to be between 200 and 600 nm, which is adequate to entrapping larger molecules or particles (DODERO et al., 2018).

One strategy that could change this scenario is the partial oxidation of HA. Periodate oxidation opens the d-glucuronic ring, creating two aldehyde groups, providing flexibility, alignment of the chains and compaction of the HA structure. The partial oxidation also makes possible the HA crosslinking with adipic dihydrazide (ADH) without external sources of energy and catalysts (TAN et al., 2009). Advantages of this crosslinking by click reaction are no toxic byproducts formation and metabolization of ADH by the organism (LI et al., 2014; SU; CHEN; LIN, 2010). Furthermore, the gelation of HA/ADH is thermo-sensitive, allowing improved injectability and in situ gelation without the necessity of any source of external energy (ITO et al., 2007).

This work aimed to study the stability of hydrogels of oxidized hyaluronic acid (oxi-HA) crosslinked with adipic dihydrazide and containing entrapped tempol under oxidative stress. The hydrogels were configurated in solid matrices or nano and microparticles.

Initially the ability of tempol for scavenge ABTS+• and DPPH• when in solution or associated with micro or nanoparticles was evaluated. The oxidative stress was provided by exposition to hydrogen peroxide, and HA stability analyzed by its remaining mass along the time. The obtained results are relevant to get safe formulations of long-lasting HA for medical uses. As far as we know, there are no scientific studies reported in the literature on the effects of tempol on the stability of the HA/ADH matrices under oxidative stress.

2.2. Methods

2.2.1. Production of oxi-HA

The oxidation of HA was made according to the protocol proposed by Lin et al. (2012) and Ma et al. (2017). A sodium periodate solution (10.67 % w/v, Milli-Q water) at room temperature was mixed with HA (1 % w/v, Milli-Q water) under agitation for 24 h in a beaker wrapped with aluminum foil. The molar ratios of HA: $NaIO_4$ were 1:2 and 1:3 and these oxi-HA samples were called oxi-HA2 and oxi-HA3 respectively. After 24 h, the reaction was quenched with the addition of ethylene glycol and the reaction medium was stirred for 0.5 h. The resulting solution was dialyzed for three days, replacing water at least twice daily and then the dialyzed solution was lyophilized.

2.2.2. Preparation of oxi-HA/ADH hydrogels

The oxi-HA/ADH hydrogels were also produced according to the protocol described by Lin et al. (2012) and Ma et al. (2017) with modifications. Briefly, 300 µL of oxi-HA (8 % w/v, PBS) was mixed with 100 µL of a tempol solution (5 % w/v, PBS) and then 100 µL of an ADH solution (8 % w/v, PBS) were added to the mixture. The solutions were stored for 12 h at 4 °C to obtain complete gelation. The hydrogels were named considering the 1:2 and 1:3 HA: $NaIO_4$ proportions, such as oxi-HA2 and oxi-HA3, and also the concentration of ADH for the crosslinking, 2%, 4% and 8% w/v. Therefore, a hydrogel produced with oxi-HA2 and ADH 4% w/v is called oxi-HA3/ADH4.

2.2.3. Preparation of HA microparticles

Briefly, 400 µL of oxi-HA2 (8 % w/v, PBS) was mixed with 100 µL of an ADH solution (8 % w/v, PBS) and stored at 4 °C. After 12 h, the hydrogel was sheared with a T25 digital ULTRA-TURRAX (IKA Laboritechnik, Staufen, Germany) at the speed of 21,000 rpm for 20 min. A previous study from this group determined these specifications. The solution was frozen with liquid nitrogen and lyophilized.

2.2.4. Synthesis of nanoparticles

The oxi-HA/ADH nanoparticles were produced by nanoprecipitation in ethanol, according to the protocols proposed by Hu et al. (2006) with modifications introduced by Bicudo and Santana (2012) for HA and adapted for oxi-HA/ADH hydrogels. Briefly, 10 mL of an oxi-HA2 solution (0.1 % w/v, Milli-Q water) was mixed with 250 µL of an ADH solution (2 % w/v, Milli-Q water) and the reaction medium was kept under agitation at 21 °C. Afterward, 26.75 mL of ethanol was added at the rate of 0.8 mL/s by a NE-300 "Just Infusion"™ syringe pump (New Era Pump Systems, Inc., Farmingdale, New York, United States). After 24 h, the nanoparticle dispersion was filtrated in polycarbonate membrane under nitrogen pressure, and the retentate containing the nanoparticles was lyophilized for storing at 4 °C.

2.2.5. Swelling and tempol incorporation capacity of micro and nanoparticles

To quantify the microparticle's swelling capacity they were previously weighted on a Petri dishes, followed by Milli-Q water addition by dropping up to saturation. The wet particles were weighted, and the swelling capacity was calculated by Eq. 1:

$$\text{Swelling (\%)} = 100 * (wf - wp)/wf \qquad (1)$$

Where wp is the weight of dry particles and wf is the weight of wet particles.

To quantifying the incorporation of tempol into the nanoparticles the swelling protocol was followed, using a tempol solution (500 mg/mL, PBS). The entrapment of tempol was calculated according to the Eq. 2:

$$\text{Tempol incorporation (g/g)} = wt/wp \qquad (2)$$

Where wt is the weight of tempol added to the particles.

2.2.6. Preparation of hydrogels/particles mixture

In order to produce hydrogels associated with particles, the protocol described in the item 2.2.2 was slightly modified. The swollen particles were dissolved in PBS in order to obtain a 50 mg/mL tempol solution. After that, 100 µL of these particles + tempol solution were mixed with 300 µL of oxi-HA (8 % w/v, PBS) and finally, 100 µL of ADH (4 or 8 % w/v, PBS) were added to the mixture. The hydrogels were also stored at 4 °C.

2.2.7. Characterization of oxi-HA

The oxidation degree of oxi-HA samples was quantified using a TNBS assay [15]. Briefly, 25 µL of t-BC (30 mM, 1 % aqueous trichloroacetic acid) was added to 25 µL of oxi-HA (0.6 %, Milli-Q water), and the mixture was kept at room temperature for 24 h. After 24 h, 0.5 mL of aqueous TNBS solution (6 mM, 0.1 M borate buffer) was transferred to an Eppendorf tube to react with the excess t-BC for 60 minutes at room temperature. Then, this solution was diluted with 0.5 N hydrochloric acid so the absorbance of the solution could be measured with a Genesys 6 spectrophotometer (Thermo Fisher Scientific, Massachusetts, USA) at 330 nm. A t-BC analytical curve with concentrations ranging from 5 to 30 mM was used. All experiments were performed in triplicate.

2.2.8. Characterization of microparticles

A Long Bench-MAM 5005 Mastersizer-S (Malvern Panalytical, Malvern, United Kingdom) was used to quantify the average diameter and size distribution of the microparticles. The measurements were made in a Sample Suspension Unit with agitation and pumping of 2.400 rpm.

2.2.9. Characterization of nanoparticles

The hydrodynamic mean dynamic diameter and polydispersity index of the nanoparticles, Z-average and PDI, were quantified by dynamic light scattering using a Zetasizer Nano ZS (Malvern Panalytical, United Kingdom). The measurements were made in triplicate using a Ne-He laser and a scattering angle of 90°. The CONTIN algorithm was used to estimate size distribution (PROVENCHER, 1982) and Z-average values were calculated according to Eq. 3 (KOPPEL, 1972).

$$Dz = (\sum ci \times mi \times Di)/(\sum ci \times mi) \qquad (3)$$

Where Dz is the z-average value, ci is the weight concentration, mi is the MM and Di is the diameter of the particle.

Zeta potential was also measured with a Zetasizer Nano ZS and the same concentration of 0.1 % (w/v) at 25ºC, using an optical path of 1 cm.

2.2.10. Antioxidant assays

The free radical scavenging potential of tempol, microparticles and nanoparticles was calculated throughout 25 days using two spectrophotometric methods: $ABTS^{+\bullet}$ and $DPPH^{\bullet}$.

Ascorbic acid was used as a positive control due to its well documented antioxidant activity (CANDAN et al., 2003; GÜLÇIN, 2007). The results were given as the percentage of radical scavenging.

2.2.10.1. DPPH assay

This decolorization assay was performed according to the procedure proposed by Blois (1958) with modifications. Briefly, a $DPPH^{\bullet}$ solution (0.1 mM, ethanol) was diluted until an absorbance of 1.05 ± 0.01 was obtained at 517 nm. Then, 2 mL of the diluted $DPPH^{\bullet}$ solution was mixed with 0,6 mL of a 350 µg/mL antioxidant solution and the sample's absorbance at 517 nm was recorded after 30 min. The sample's absorbance was recorded every day for 25 days. The $DPPH^{\bullet}$ scavenging of each sample was calculated using Equation 4:

$$DPPH^{\bullet} \text{ scavenging } (\%) = [1 - (As/Ab)] \times 100 \qquad (4)$$

Where As and Ab are the absorbances of $DPPH^{\bullet}$ in the presence and absence of the scavenger, respectively.

2.2.10.2. ABTS assay

This decolorization assay was performed according to the procedure proposed by Re et al. (1999) with modifications. Briefly, ABTS (7 mM, Milli-Q water) was mixed with potassium persulfate (2.45 mM, Milli-Q water) for 16 h in a dark environment in order to produce the free radical $ABTS^{+\bullet}$. Then the free radical solution was diluted until an absorbance of 0.70 ± 0.01 at 734 nm was obtained. Lastly, 1.7 mL of the diluted $ABTS^{+\bullet}$ solution was then mixed with 0.3 mL of a 350 µg/mL antioxidant solution and the sample's absorbance was recorded at 734 nm after 30 min. The sample's absorbance was recorded every day for 25 days. The $ABTS^{+\bullet}$ scavenging of each sample was calculated using Equation 5:

$$ABTS^{+\bullet} \text{ scavenging } (\%) = [1 - (As/Ab)] \times 100 \qquad (5)$$

Where As and Ab are the absorbances of $ABTS^{+\bullet}$ in the presence and absence of the scavenger, respectively.

2.2.11. Release of tempol

The profiles of tempol release were constructed by measuring the antioxidant's concentration in PBS in time intervals until the equilibrium was reached. Each hydrogel produced in the presence of tempol were submerged in PBS inside an Eppendorf which had its lid removed. A dialysis membrane (MWCO of 12,000-16,000 Da) was used to cover the Eppendorf's open end, and the Eppendorf was put inside a falcon tube which had PBS in so that the membrane was slightly submerged in the PBS. The concentration of the PBS outside of the Eppendorf was the one that was measured during the assay using a Thermo Electron Spectronic GENESYS 6 UV-Visible Spectrophotometer (Waltham, Massachusetts, United States. The same procedure was repeated with the swollen micro and nanoparticles. A previously constructed analytical curve using concentrations of tempol ranging from 0.3 to 2 mg/mL at 428 nm was used.

2.2.12. Stability of oxi-HA/ADH hydrogels associated with tempol under oxidative stress

The ratios between the remaining mass of the hydrogels in each day and the initial mass of each sample were used to study the degradation under oxidative stress, which was induced by a 100 µmol/L H_2O_2 solution. Each day, for 25 days, the hydrogels were removed from the H_2O_2 solution, the water excess was removed with a piece of a paper filter, and they were weighted. Hydrogels without tempol in PBS and a 100 µmol/L H_2O_2 solution were used as controls.

2.2.13. Degradation of nanoparticles

The nanoparticles were divided into three groups: one dispersed in PBS and the other two groups (empty nanoparticles or containing tempol) were dispersed in a 100 µmol/L H_2O_2 solution. The degradation profiles were constructed by measuring their mean Z-average, PDI and zeta potential along 25 days.

3. Results and discussion

3.1. Oxidation degree and particles characterization

The oxidation degrees of oxi-HA2 and oxi-HA3 were found to be 65 ± 5 and 82 ± 5 %, respectively. Table 1 shows the physicochemical properties and entrapped tempol for the oxi-HA/ADH hydrogels configurated in a solid matrix and micro or nanoparticles.

Table 1. Characterization of micro and nanoparticles.

	Microparticles	Nanoparticles
Average mean diameter	255 ± 22 µm	152 ± 11 nm
Z-average (nm)	-	182 ± 2
PDI	-	0.22 ± 0.02
Zeta potential (mV)	-	- 65 ± 4 mV
Swelling (%)	93.6 ± 0.5	95 ± 1
Tempol incorporation (g of tempol/g of particles)	7.4 ± 0.7	11 ± 3

Although nanoparticles have demonstrated more significant swelling values, the microparticles have an expressive value of swelling as well. The same is true for the tempol absorption, since both particles entrapped tempol in the same order of magnitude.

3.2. Radical scavenge ability of tempol, HA microparticles and HA nanoparticles

Figure 1a and 1b show the ability for $ABTS^{+\bullet}$ and $DPPH^{\bullet}$ radical scavenge along 8 days. After the 8th day, there were changes in absorbance of the solutions out of the patterns indicating degradation.

Figure 1. $ABTS^{+\bullet}$ (a) and $DPPH^{\bullet}$ (b) scavenging of tempol, ascorbic acid, microparticles and nanoparticles.

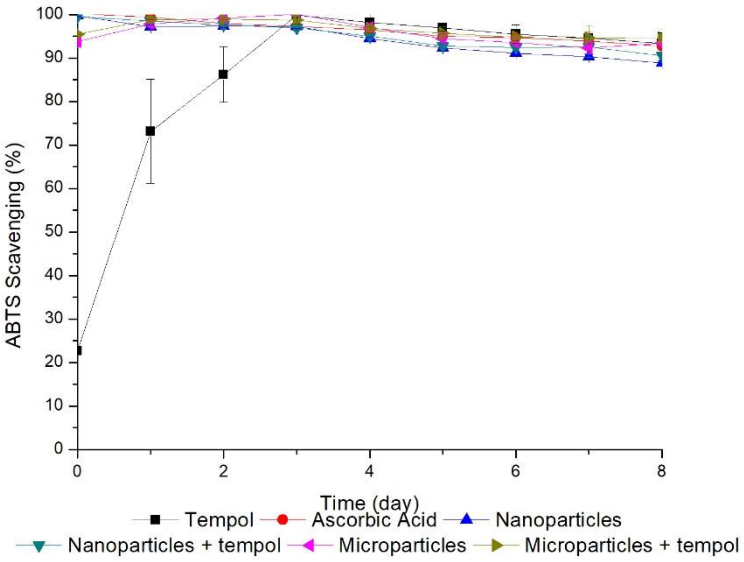

(a)

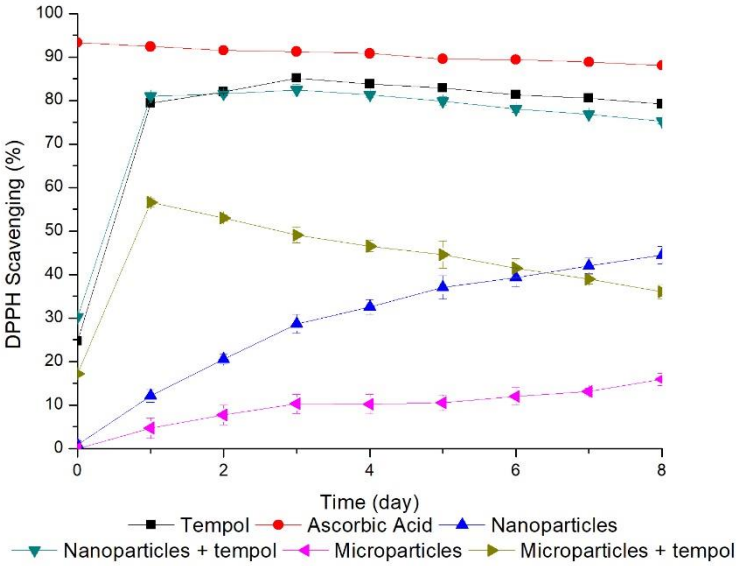

(b)

There are two paths in which antioxidants can react with free radicals: by electron transfer and by H-atom transfer. In the first, the antioxidant can transfer an electron to the free radical becoming itself a radical, while in the later hydrogen is removed from the antioxidant by the radical (WRIGHT; JOHNSON; DILABIO, 2001).

The $ABTS^{+\bullet}$ method involves an electron-transfer path represented by the following reaction:

$$ABTS^{+\bullet} + R\text{-}XH \rightarrow ABTS+ + R\text{-}X^{\bullet}$$

In neutral pH, a fraction of phenolic and carboxylic groups deprotonates transferring protons to the medium. This behavior allows the HA matrices which have a negative charge, to transfer electrons to ABTS+• and form stable radicals. According to the Figure 2a, tempol scavenge ABTS+• slower due to its redox-recycle reactions, since tempol can alternate in three different stable free radicals by undergoing one electron transfer reaction (KRISHNA et al., 1992, 1996a, 1996b). Figure 2 shows the redox-recycling reactions of tempol molecules. Every specimen, except free tempol, had ABTS+• scavenging values higher than 88 % from the starting day, while free tempol only reached 80 % radical scavenging after the second day of reaction with ABTS+•. These results show that micro and nanoparticles had a vital performance on free radical scavenging even when they were not associated with tempol.

Figure 2. Scheme of the redox-recycling of tempol molecules.

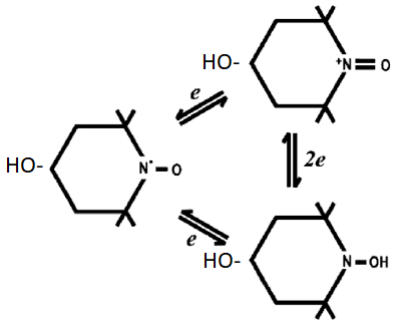

Antioxidants can scavenge $DPPH^{\bullet}$ via two different paths: H atom transfer or proton concerted electron-transfer process (a and b, respectively) (LITWINIENKO; INGOLD, 2003; WANG; ZHANG, 2003).

$$DPPH^{\bullet} + R\text{-}XH \rightarrow DPPHH + RX^{\bullet} \quad (a)$$

$$DPPH^{\bullet} + RXH \rightarrow DPPH\text{-} + RXH^{+\bullet} \rightarrow DPPHH + RX^{\bullet} \quad (b)$$

Where X can represent O, N, C or S (LITWINIENKO; INGOLD, 2003; WANG; ZHANG, 2003).

DPPH• is less reactive than ABTS+• due to the steric hindrance around the N atom that makes difficult the transfer of H-atom from the antioxidant to the radical (FOTI, 2015), which may explain why the nanoparticles without tempol had higherDPPH• scavenge values than the microparticles. Although both types of particles had lower values of the free radical scavenger, the nanoparticles presented better performance tendency. Since the nanoparticles have a bigger surface area, there are more groups available for electron or H atom transfer, while the microparticles need the DPPH• to diffuse inside them to react with the free radicals. The reaction between tempol and DPPH• is slower than with ascorbic acid, but after 24 h, tempol had radical scavenging ability higher than 79 %.

3.3. Tempol's release

Figures 3a, 3b and 3c show the concentration of tempol released from the solid hydrogel matrices alone or containing micro or nanoparticles. It could be observed, the equilibrium was reached under 6 h in all hydrogels or swollen particles, with differences in the initial rates of release in the oxi-HA3/ADH8, oxi-HA3/ADH8 + nanoparticles, and free nanoparticles. This difference is likely linked to the fact that the hydrogel oxi-HA3/ADH8 has a higher crosslinking degree and the fact that in the oxi-HA3/ADH8 + nanoparticles hydrogel the tempol molecules have to go from the nanoparticles to the hydrogel matrix and then to the PBS solution, having to face more mass transfer barriers.

Figure 3. Release of tempol from oxi-HA/ADH hydrogels without particles (a), associated with nanoparticles (b) and associated with microparticles (c).

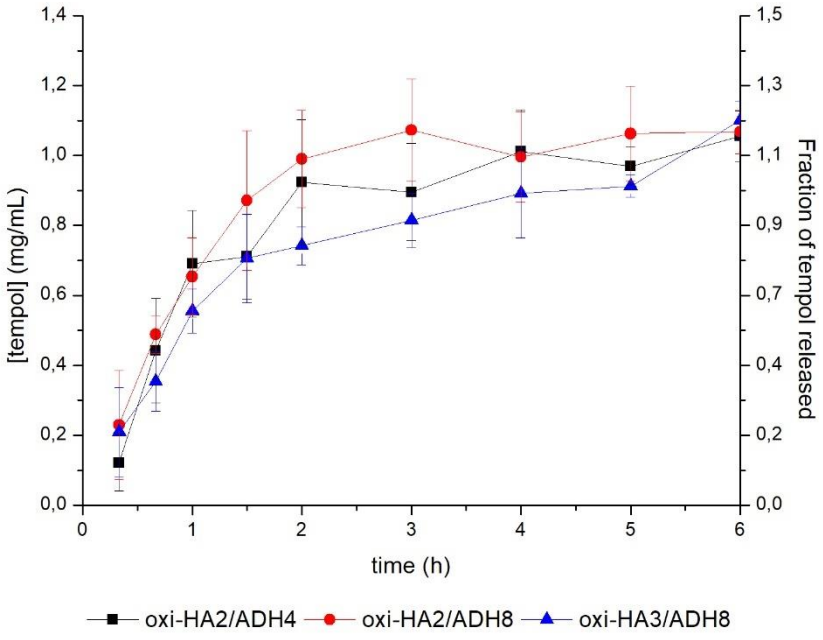

(a)

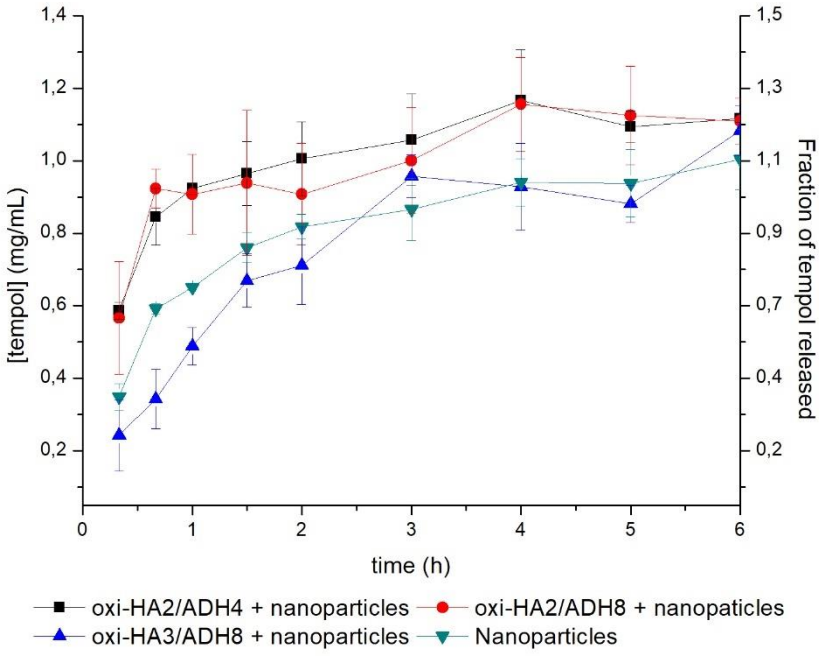

(b)

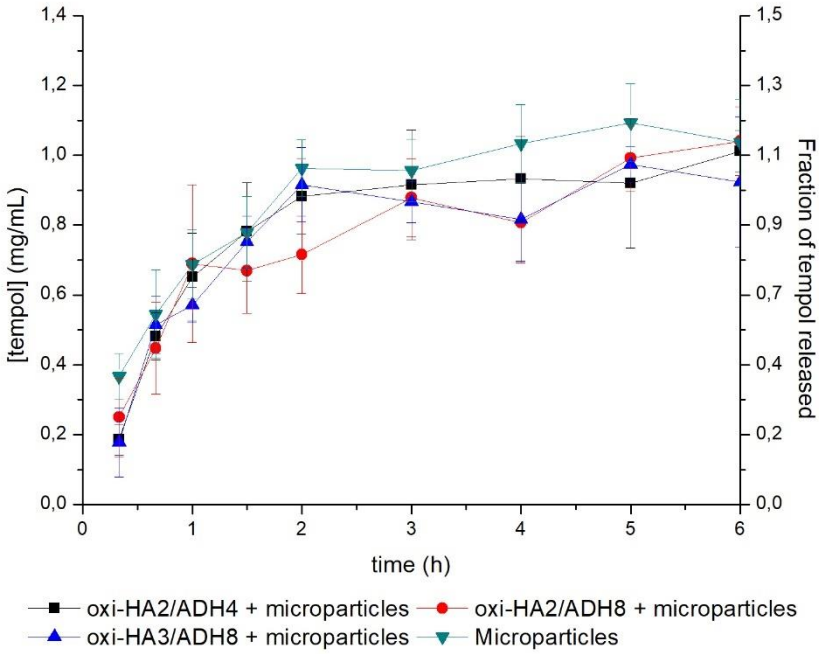

(c)

3.4. Degradation under oxidative stress

Figure 4a 4b and 4c show the degradation profiles of the hydrogels during 25 days under induced oxidative stress. Degradation was quantified in terms of the ratios between their actual and initial masses. It can be observed that under oxidative stress, all hydrogels were swollen such that their masses were increased compared to the initial ones. The effects were inverse in the presence of PBS, due to the changes into the matrices caused by the presence of the buffer or hydrogen peroxide.

Figure 4. Degradation profiles of oxi-HA2/ADH4 (a), oxi-HA2/ADH8 (b) and oxi-HA3/ADH8 (c).

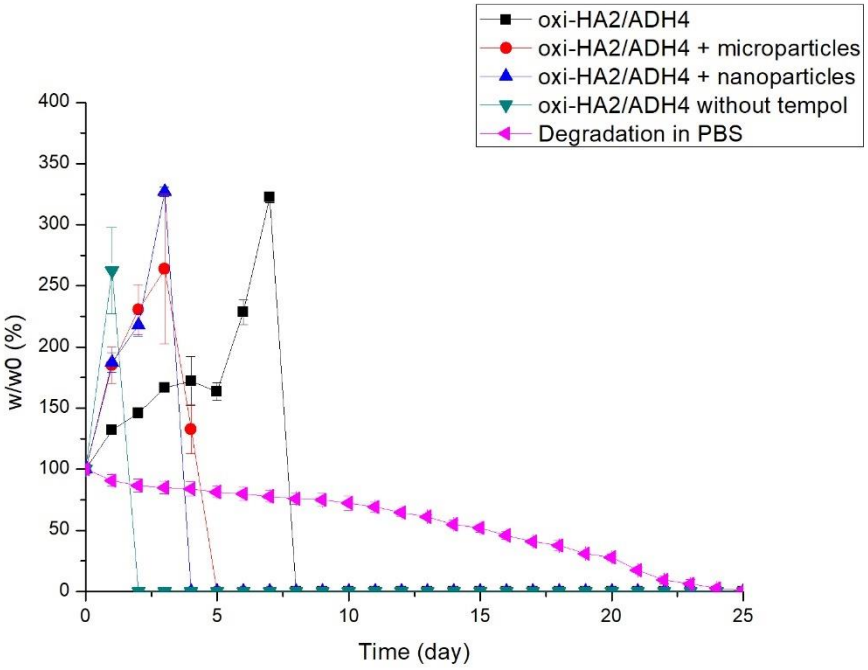

(a)

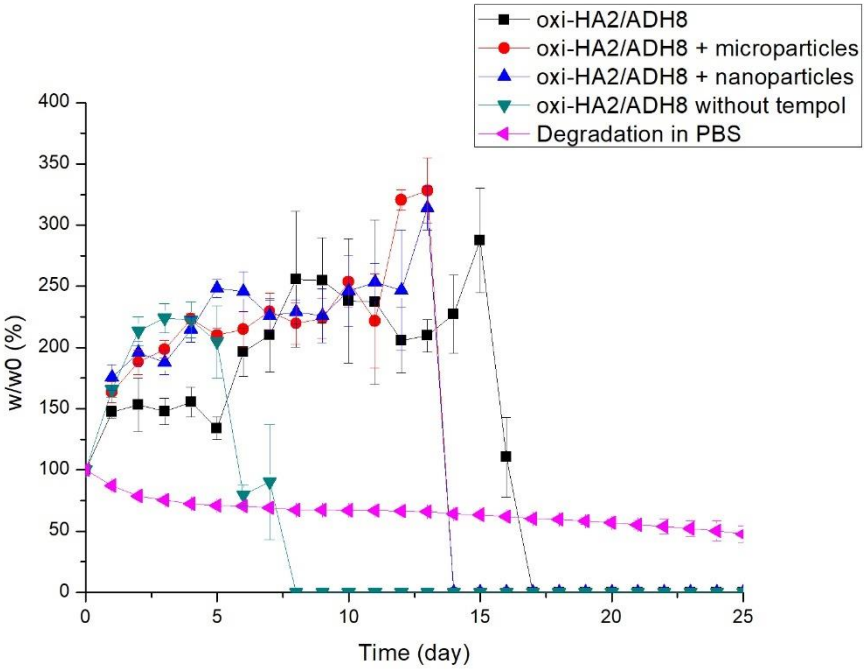

(b)

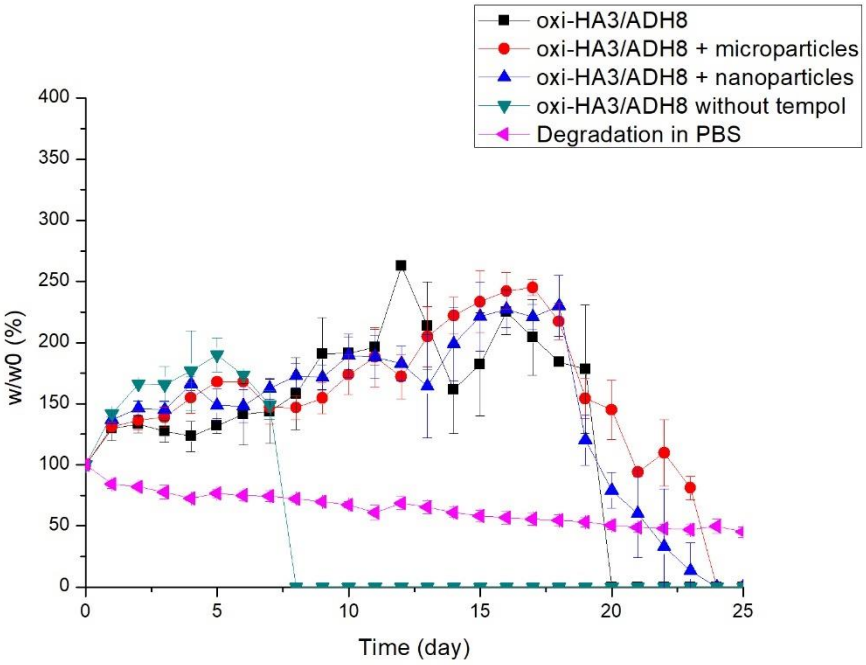

(c)

Under oxidative stress, oxi-HA2/ADH4 completely dissolved under 8 days, with or without any kind of particles, while the same hydrogel without the presence of tempol dissolved after 24 h. Oxi-HA2/ADH8 under oxidative stress lasted between 13 and 16 days with or without the association with particles and oxi-HA3/ADH8 lasted between 19 and 23 days, while those hydrogels without tempol lasted respectively 7 and 8 days. These results show the positive impact of tempol on protection of the matrices against the attack of free radicals produced in the induced oxidative stress.

In relation to the presence of micro and nanoparticles, only in oxi-HA3/ADH8 their effects could be observed due to its stability along time.

Therefore, the higher crosslinking extension of the oxi-HA3/ADH8 enhance the stability provided by tempol, due to the resistance to degradation provided by the higher extension of ADH crosslinking as well as due to the presence of charges and the smallest domains in the matrices that limited the extent of the hydrogen peroxide attack.

Figure 5 shows Z-average (a), PDI (b) and zeta potential (c) of nanoparticles dissolved in Milli-Q water, H_2O_2 and H_2O_2 + tempol for 25 days. Throughout the 25 days the nanoparticles under the three different conditions had the same behavior. All samples slightly tend to increase their values of Z-average and PDI, while the zeta potential values tend to approach lower values in module. The high zeta potential values in module are responsible for

the stability of the nanoparticles in water, while the stability in H_2O_2 can be explained by the antioxidant properties presented in the work and the presence of tempol, when it is added to the particles. The increase in the Z-average and PDI values can be related to the tendency of coalescence and aggregation of smaller particles, producing bigger ones over time. Even so, the three nanoparticles samples still have relatively low values of PDI.

Figure 5. Z-average (a), PDI (b) and zeta potential (c) of nanoparticles dissolved in Milli-Q water, H_2O_2 and H_2O_2 + tempol for 25 days.

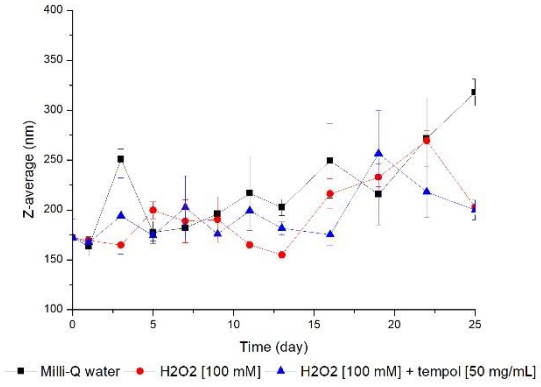

(a)

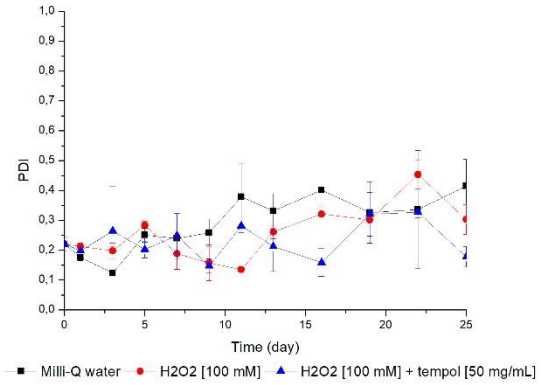

(b)

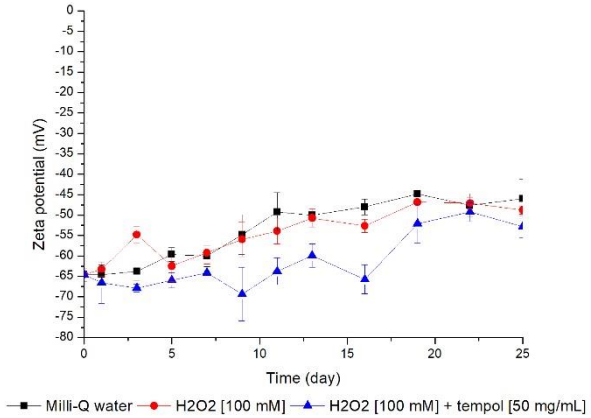

(c)

4. Conclusions

In this work, oxi-HA/ADH hydrogels configurated in solid matrices and micro and nanoparticles were successfully produced incorporating tempol by swelling. Although the better stability produced by the entrapped tempol into the structures, compared with the effects of ADH crosslink alone, the extension of the crosslinking enhanced the antioxidant action of

tempol. Therefore, the best results were obtained with the oxi-HA3/ADH8 prepared from oxi-HA3, ADH 8 %. The protective effects were enhanced by the addition of nano or microparticles to the solid oxi-HA3/ADH8 matrix. These results open perspectives for optimization of long-lasting HA formulations, as well as extend its application for drug delivery, entrapping of stem cells and bioprinting of biological structures for medical applications.

Author contributions

All authors contributed to the conception and design of this study and to the acquisition and analysis of the data. All authors contributed to the drafting and revising of this article and have approved the final version to be submitted.

Acknowledgments

This work was supported by the National Council for Scientific and Technological Development (process 10924/2017-5 and 153611/2016-2).

5. References

BALAZS, E.; DENLINGER, J. Viscosupplementation: a new concept in the treatment of osteoarthritis. **The Journal of Rheumatology**, v. 20, p. 3–9, 1993.

BICUDO, R. C. S.; SANTANA, M. H. A. Effects of Organic Solvents on Hyaluronic Acid Nanoparticles Obtained by Precipitation and Chemical Crosslinking. **Journal of Nanoscience and Nanotechnology**, v. 12, n. 13, p. 2849–2857, 2012.

BLOIS, M. . Antioxidant Determinations by the Use of a Stable Free Radical. **Nature**, v. 181, p. 1199–1200, 1958.

BROCKMEIER, S. F.; SHAFFER, B. S. Viscosupplementation Therapy for Osteoarthritis. **Sports Medicine and Arthroscopy Review**, v. 14, n. 3, p. 155–162, 2006.

CANDAN, F. et al. Antioxidant and antimicrobial activity of the essential oil and methanol extracts of Achillea millefolium subsp. millefolium Afan. (Asteraceae). **Journal of Ethnopharmacology**, v. 87, n. 2–3, p. 215–220, 2003.

DODERO, A. et al. Characterization of hyaluronic acid by dynamic light scattering and rheological techniques. **AIP Conference Proceedings**, v. 1981, 2018.

DOS SANTOS, A. B. et al. Antioxidant properties of plant extracts: An EPR and DFT comparative study of the reaction with DPPH, TEMPOL and spin trap DMPO. **Journal of the Brazilian Chemical Society**, v. 20, n. 8, p. 1483–1492, 2009.

FOTI, M. C. Use and Abuse of the DPPH• Radical. **Journal of Agricultural and Food Chemistry**, v. 63, p. 8765−8776, 2015.

GARG, H. G.; HALES, C. A. **Chemistry and Biology of Hyaluronan**. Boston: Elsevier B.V., 2004.

GÜLÇIN, I. Comparison of *in vitro* antioxidant and antiradical activities of L-tyrosine and L-Dopa. **Amino Acids**, v. 32, n. 3, p. 431–438, 2007.

HU, Z.; XIA, X.; TANG, L. **PROCESS FOR SYNTHESIZING OIL AND SURFACTANT-FREE HYALURONCACD NANOPARTICLES AND MICROPARTICLES**. United States, 2009.

ITO, T. et al. The prevention of peritoneal adhesions by *in situ* cross-linking hydrogels of hyaluronic acid and cellulose derivatives. **Biomaterials**, v. 28, p. 975–983, 2007.

KOPPEL, D. E. Analysis of macromolecular polydispersity in intensity correlation spectroscopy: The method of cumulants. **The Journal of Chemical Physics**, v. 57, n. 11, p. 4814–4820, 1972.

KRISHNA, M. C. et al. Oxoammonium cation intermediate in the nitroxide-catalyzed dismutation of superoxide. **Proceedings of the National Academy of Sciences**, v. 89, n. 12, p. 5537–5541, 1992.

KRISHNA, M. C. et al. Stimulation by nitroxides of catalase-like activity of hemeproteins. Kinetics and mechanism. **Journal of Biological Chemistry**, v. 271, n. 42, p. 26018–26025, 1996a.

KRISHNA, M. C. et al. Do nitroxide antioxidants act as scavengers of O2/-· or as SOD mimics? **Journal of Biological Chemistry**, v. 271, n. 42, p. 26026–26031, 1996b.

LI, L. et al. Biodegradable and injectable *in situ* cross-linking chitosan-hyaluronic acid based hydrogels for postoperative adhesion prevention. **Biomaterials**, v. 35, n. 12, p. 3903–3917, 2014.

LIN, F.-H. et al. **CROSS-LINKED OXIDATED HYALURONIC ACID FOR USE ASA VITREOUS SUBSTITUTE**. United States, 2012.

LITWINIENKO, G.; INGOLD, K. U. Abnormal Solvent Effects on Hydrogen Atom Abstractions . 1 . The Reactions of Phenols with 2 , 2-Diphenyl-1-picrylhydrazyl (dpph •) in Alcohols. v. 68, n. **The Journal of Organic Chemistry**, p. 3433–3438, 2003.

MA, X. et al. Improvement of toughness for the hyaluronic acid and adipic acid dihydrazide hydrogel by PEG. **Fibers and Polymers**, v. 18, n. 5, p. 817–824, 2017.

PROVENCHER, S. W. A CONSTRAINED REGULARIZATION METHOD FOR INVERTING DATA REPRESENTED BY LINEAR ALGEBRAIC OR INTEGRAL EQUATIONS. **Computer Physics Communications**, v. 27, p. 213–227, 1982.

RE, R. et al. Antioxidant activity applying an improved ABTS radical cation decolorization assay. **Free Radical Biology and Medicine**, v. 26, n. 98, p. 1231–1237, 1999.

SHE, C. Y.; DINH, N. D.; TU, A. T. Laser raman scattering of glucosamine, n-acetylglucosamine, and glucuronic acid. **Biochimica et Biophysica Acta**, v. 372, p. 345–357, 1974.

SHEU, S. Y. et al. Biological characterization of oxidized hyaluronic acid/resveratrol hydrogel for cartilage tissue engineering. **Journal of Biomedical Materials Research - Part A**, v. 101, n. 12, p. 3457–3466, 2013.

SU, W. Y.; CHEN, Y. C.; LIN, F. H. Injectable oxidized hyaluronic acid/adipic acid dihydrazide hydrogel for nucleus pulposus regeneration. **Acta Biomaterialia**, v. 6, n. 8, p. 3044–3055, 2010.

TAN, H. et al. Injectable *in situ* forming biodegradable chitosan-hyaluronic acid based hydrogels for cartilage tissue engineering. **Biomaterials**, v. 30, n. 13, p. 2499–2506, 2009.

VALAVANIDIS, A. et al. Comparison of the Radical Scavenging Potential of Polar and Lipidic Fractions of Olive Oil and Other Vegetable Oils under Normal Conditions and after Thermal Treatment. **Journal of Agricultural and Food Chemistry**, v. 52, n. 8, p. 2358–2365, 2004.

WANG, L.-F.; ZHANG, H.-Y. A Theoretical Investigation on DPPH Radical-Scavenging Mechanism of Edaravone. **Bioorganic & MedicinalChemistry Letters**, v. 13, p. 3789–3792, 2003.

WATTERSON, J.; ESDAILE, J. Viscosupplementation: therapeutic mechanisms and clinical potential in osteoarthritis of the knee. **Journal of the American Academy of Orthopaedic Surgeons**, v. 8, n. 277–284, 2000.

WRIGHT, J. S.; JOHNSON, E. R.; DILABIO, G. A. Predicting the activity of phenolic antioxidants: Theoretical method, analysis of substituent effects, and application to major families of antioxidants. **Journal of the American Chemical Society**, v. 123, n. 6, p. 1173–1183, 2001.

YEN, G. C.; CHEN, H. Y. Antioxidant Activity of Various Tea Extracts in Relation to Their Antimutagenicity. **Journal of Agricultural and Food Chemistry**, v. 43, n. 1, p. 27–32, 1995.

5 CONCLUSÃO GERAL

A oxidação parcial do AH permite a produção de hidrogéis com propriedades físico-químicas capazes de beneficiarem a sua reticulação *in situ* com ADH, além de modularem taxas iniciais de liberação de tempol, em hidrogéis sólidos e configurados em nano e micropartículas. A presença do tempol nos hidrogéis reticulados lhes conferiu maior proteção contra o stress oxidativo, abrindo perspectivas para o projeto e a produção de formulações de AH mais estáveis para aplicações *in vivo*.

Os resultados deste trabalho contribuem para o desenvolvimento de novos biomateriais uteis para aplicações em engenharia de tecidos e tratamento de doenças ortopédicas.

6. SUGESTÕES PARA TRABALHOS FUTUROS

- Realização de ensaios de proliferação celular em hidrogéis de oxi-AH/ADH para avaliação de viabilidade celular e toxicidade;
- Ensaios *in vivo* de maneira a verificar os efeitos dos *scaffolds* em modelos animais;
- Associação dos hidrogéis de oxi-AH/ADH contendo tempol com Plasma Rico em Plaquetas (PRP), um promissor biomaterial relacionado à medicina regenerativa;

REFERÊNCIAS BIBLIOGRÁFICAS

ALLEMANN, I. B.; BAUMANN, L. Hyaluronic acid gel (Juvéderm^{TM}) preparations in the treatment of facial wrinkles and folds. **Clinical Interventions in Aging**, v. 3, n. 4, p. 629–634, 2008.

BALAZS, E. A.; LESHCHINER, A. **Cross-Linked Gels of Hiyaluronic Acid and Products Containing Such Gels**, 1984.

BALAZS, E.; DENLINGER, J. Viscosupplementation: a new concept in the treatment of osteoarthritis. **The Journal of Rheumatology**, v. 20, p. 3–9, 1993.

BUFFA, R. et al. **METHOD OF PREPARATION OF AN OXIDIZED DERIVATIVE OF HYALURONIC ACID AND A METHOD OF MODIFICATION THEREOF**United States, 2012.

BURTON, G.; INGOLD, K. Living organisms are exposed to much more severe oxidation than is food in a refrigerator. Nevertheless, they do not become rancid until they, in their turn, become food. In: HALLIWELL, B.; GUTTERIDGE, J. M. C. (Eds.). . **Free Radicals in Biology and Medicine**. Quinta Edi ed. Oxford: Oxford University Press, 2015. p. 77–152.

CAI, Y. et al. A hyaluronic acid-based hydrogel enabling CD44-mediated chondrocyte binding and gapmer oligonucleotide release for modulation of gene expression in osteoarthritis. **Journal of Controlled Release**, v. 253, p. 153–159, 2017.

CAMPOCCIA, D. et al. Semisynthetic resorbable materials from hyaluronan esterification. **Biomaterials**, v. 19, p. 2101–2127, 1998.

CHATTERJEE, P. K. et al. Tempol, a membrane-permeable radical scavenger , reduces oxidant stress-mediated renal dysfunction and injury in the rat. **Kidney International**, v. 58, p. 658–673, 2000.

CHEN, F. M.; LIU, X. Advancing biomaterials of human origin for tissue engineering. **Progress in Polymer Science**, v. 53, p. 86–168, 2016.

CHONG, B. F. et al. Microbial hyaluronic acid production. **Applied Microbiology and Biotechnology**, v. 66, n. 4, p. 341–351, 2005.

CLEARY, P. P.; LARKIN, A. Hyaluronic Acid Capsule : Strategy for Oxygen Resistance in Group A Streptococci. **Journal of Bacteriology**, v. 140, n. 3, p. 1090–1097, 1979.

COLLINS, M. N.; BIRKINSHAW, C. Comparison of the Effectiveness of Four Different Crosslinking Agents with Hyaluronic Acid Hydrogel Films for Tissue-Culture Applications.

Journal of Applied Polymer Science, v. 104, p. 3183–3191, 2007.

COLLINS, M. N.; BIRKINSHAW, C. Physical properties of crosslinked hyaluronic acid hydrogels. **Journal of Materials Science: Materials in Medicine**, v. 19, n. 11, p. 3335–3343, 2008.

CRESCENZI, V.; FRANCESCANGELI, A. Note: Biological activity of C6-oxidized hyaluronic acid: Antibacterial properties of the Zn(II) salt. **Journal of Bioactive and Compatible Polymers**, v. 18, n. 3, p. 229–235, 2003.

CROSS, M. et al. The global burden of hip and knee osteoarthritis: estimates from the Global Burden of Disease 2010 study. **Annals of the Rheumatic Diseases**, v. 73, n. 7, p. 1323–1330, 2014.

DE BOULLE, K. et al. A review of the metabolism of 1,4-butanediol diglycidyl ether-crosslinked hyaluronic acid dermal fillers. **Dermatologic Surgery**, v. 39, n. 12, p. 1758–1766, 2013.

DOS SANTOS, A. B. et al. Antioxidant properties of plant extracts: An EPR and DFT comparative study of the reaction with DPPH, TEMPOL and spin trap DMPO. **Journal of the Brazilian Chemical Society**, v. 20, n. 8, p. 1483–1492, 2009.

DOUGADOS, M. et al. Prevalence of comorbidities in rheumatoid arthritis and evaluation of their monitoring: results of an international, cross-sectional study (COMORA). **Annals of the Rheumatic Diseases**, v. 73, n. 1, p. 62–68, 2014.

EVANS, N. D.; GENTLEMAN, E.; POLAK, J. M. Scaffolds for stem cells. **Materials Today**, v. 9, n. 12, p. 26–33, 2006.

FERNANDES, C. et al. Nanotechnology and Antioxidant Therapy : An Emerging Approach for Neurodegenerative Diseases. **Current Medicinal Chemistry**, v. 21, p. 4311–4327, 2014.

FRASER, J. R. F. et al. Plasma clearance, tissue distribution and metabolism of hyaluronic acid injected intravenously in the rabbit. **Biochemical Journal**, v. 200, n. 2, p. 415–424, 1981.

GARG, H. G.; HALES, C. A. **Chemistry and Biology of Hyaluronan**. Boston: Elsevier B.V., 2004.

GHOSH, S. et al. Tribological role of synovial fluid compositions on artificial joints— a systematic review of the last 10 years. **Lubrication Science**, v. 26, p. 387–410, 2014.

GRAND VIEW RESEARCH. **Hyaluronic Acid Market Analysis by Application (Dermal Fillers, Osteoarthritis [Single Injection, Three Injection, Five Injection], Ophthalmic, Vesicoureteral Reflux), by Region (North America, Europe, Asia Pacific, Latin America,**

MEA) and Segment Forecas. [s.l: s.n.].

HASCALL, V. C.; LAURENT, T. . **Hyaluronan: structure and physical properties**. Disponível em: <http://glycoforum.gr.jp/science/hyaluronan/HA01/HA01E.html>. Acesso em: 9 out. 2017.

HOKPUTSA, S. et al. Hydrodynamic characterisation of chemically degraded hyaluronic acid. **Carbohydrate Polymers**, v. 52, n. 2, p. 111–117, 2003.

IANNITTI, T. et al. A new highly viscoelastic hyaluronic acid gel: Rheological properties, biocompatibility and clinical investigation in esthetic and restorative surgery. **International Journal of Pharmaceutics**, v. 456, n. 2, p. 583–592, 2013.

IDATA RESEARCH INC. **Hyaluronic Acid Products from Genzyme, Sanofi-Aventis Preferred Among Orthopedic Surgeons, According to Survey.** Disponível em: <http://www.prnewswire.com/news-releases/hyaluronic-acid-products-from-genzyme-sanofiaventis-preferred-among-orthopedic-surgeons-according-to-survey-118831014.html>. Acesso em: 9 out. 2017.

INGR, M.; KUTÁLKOVÁ, E.; HRNČIŘÍK, J. Hyaluronan random coils in electrolyte solutions—a molecular dynamics study. **Carbohydrate Polymers**, v. 170, p. 289–295, 2017.

JIA, X. et al. Prolongation of sciatic nerve blockade by *in situ* cross-linked hyaluronic acid. **Biomaterials**, v. 25, n. 19, p. 4797–4804, 2004.

KOLB, H. C.; FINN, M. G.; SHARPLESS, K. B. Click Chemistry: Diverse Chemical Function from a Few Good Reactions. **Angewandte Chemie - International Edition**, v. 40, n. 11, p. 2004–2021, 2001.

KRISHNA, M. C. et al. Oxoammonium cation intermediate in the nitroxide-catalyzed dismutation of superoxide. **Proceedings of the National Academy of Sciences**, v. 89, n. 12, p. 5537–5541, 1992.

KRISTIANSEN, K. A.; DALHEIM, M. Ø.; CHRISTENSEN, B. E. Periodate oxidation and macromolecular compaction of hyaluronan. **Pure and Applied Chemistry**, v. 85, n. 9, p. 1893–1900, 2013.

LAI, V. K. et al. **Swelling of Collagen-Hyaluronic Acid Co-Gels: An *In Vitro* Residual Stress ModelAnnals of Biomedical Engineering**. [s.l: s.n.].

LEACH, J. B.; SCHMIDT, C. E. Hyaluronan. In: **Encyclopedia of Biomaterials and Biomedical Engineering**. New York: Marcel Dekker, 2004. p. 779–789.

LEONG, K. F. et al. Engineering functionally graded tissue engineering scaffolds. **Journal of**

the Mechanical Behavior of Biomedical Materials, v. 1, n. 2, p. 140–152, 2008.

LI, N. N.; FU, C. P.; ZHANG, L. M. Using casein and oxidized hyaluronic acid to form biocompatible composite hydrogels for controlled drug release. **Materials Science and Engineering C**, v. 36, n. 1, p. 287–293, 2014.

LI, W. J. et al. A three-dimensional nanofibrous scaffold for cartilage tissue engineering using human mesenchymal stem cells. **Biomaterials**, v. 26, n. 6, p. 599–609, 2005.

LIN, F.-H. et al. **Cross-linked oxidated hyaluronic acid for use as a vitreous substitute**Estados Unidos, 2011.

LIN, F.-H. et al. **CROSS-LINKED OXIDATED HYALURONIC ACID FOR USE ASA VITREOUS SUBSTITUTE**United States, 2012.

LIU, L. et al. Microbial production of hyaluronic acid: current state, challenges, and perspectives. **Microbial Cell Factories**, v. 10, n. 1, p. 99, 2011.

LYUBLINSKAYA, O. G. et al. Reactive oxygen species are required for human mesenchymal stem cells to initiate proliferation after the quiescence exit. **Oxidative Medicine and Cellular Longevity**, v. 2015, p. 8, 2015.

MA, X. et al. Improvement of toughness for the hyaluronic acid and adipic acid dihydrazide hydrogel by PEG. **Fibers and Polymers**, v. 18, n. 5, p. 817–824, 2017.

MAISONNEUVE, C. D. LA; MARTINS, J. O. Public spending on health and long-term care: a new set of projections. **OECD Economic Policy Papers**, v. 6, n. 06, p. 1–39, 2013.

MALEKI, A.; KJØNIKSEN, A. L.; NYSTRÖM, B. Effect of pH on the behavior of hyaluronic acid in dilute and semidilute aqueous solutions. **Macromolecular Symposia**, v. 274, n. 1, p. 131–140, 2008.

MATSUMURA, G.; HERP, A.; PIGMAN, W. Depolymerization of Hyaluronic Acid by Autoxidants and Radiations. **Radiation Research**, v. 28, n. 4, p. 735–752, 1966.

MEDINA, J. M.; THOMAS, A.; DENEGAR, C. R. Knee osteoarthritis: Should your patient opt for hyaluronic acid injection? **Journal of Family Practice**, v. 55, n. 8, p. 669–675, 2006.

MEYER, K.; PALMER, J. W. Polysaccharide of Vitreous Humor. **Journal of Biological Chemistry**, v. 107, p. 629–634, 1934.

MODAWAL, A. et al. Hyaluronic acid injections relieve knee pain. **The Journal of Family Practice**, v. 54, n. 9, p. 758–767, 2005.

MUNNÉ-BOSCH, S.; PINTÓ-MARIJUAN, M. Free radicals, oxidative stress and antioxidants. In: THOMAS, B.; MURRAY, B. G.; MURPHY, D. J. (Eds.). . **Encyclopedia of**

Applied Plant Sciences - Volume 1. Segunda ed. [s.l.] Elsevier, 2017. p. 16–19.

MURPHY, C. M. et al. Cell scaffold interactions in the bone tissue engineering triad. **European cells & materials**, v. 26, p. 120–132, 2013.

NAIR, S. et al. A biodegradable *in situ* injectable hydrogel based on chitosan and oxidized hyaluronic acid for tissue engineering applications. **Carbohydrate Polymers**, v. 85, n. 4, p. 838–844, 2011.

NECAS, J. et al. Hyaluronic acid (hyaluronan): A review. **Veterinarni Medicina**, v. 53, n. 8, p. 397–411, 2008.

NEO, H. et al. The Effect of Hyaluronic Acid on Experimental Temporomandibular Joint Osteoarthrosis in the Sheep. **Journal of Oral and Maxillofacial Surgery**, v. 56, p. 1114–1119, 1997.

PAINTER, T.; LARSEN, B. A further illustration of nearest-neighbour auto-inhibitory effects in the oxidation of alginate by periodate ion. **Acta Chemica Scandinavica**, v. 27, p. 1957–1962, 1973.

PALMIERI-SMITH, R. M. et al. The Role of Athletic Trainers in Preventing and Managing Posttraumatic Osteoarthritis in Physically Active Populations: a Consensus Statement of the Athletic Trainers' Osteoarthritis Consortium. **Journal of Athletic Training**, v. 52, n. 6, p. 610–623, 2017.

PAN, N. C. et al. Ácido Hialurônico: Características, Produção Microbiana E Aplicações Industriais. **BBR - Biochemistry and Biotechnology Reports**, v. 2, n. 4, p. 42, 2013.

PRESTWICH, G. D. **Biomaterials from chemical-modified hyaluronan.** Disponível em: <http://glycoforum.gr.jp/science/hyaluronan/HA18/%0AHA18E.html>.

QAZI, T. H. et al. Biomaterials based strategies for skeletal muscle tissue engineering: Existing technologies and future trends. **Biomaterials**, v. 53, p. 502–521, 2015.

RAMAMURTHI, A.; VESELY, I. Smooth muscle cell adhesion on crosslinked hyaluronan gels. **J Biomed Mater Res**, v. 60, n. 1, p. 195–205, 2002.

REGAN, M. O. et al. Molecular mechanisms and genetics of hyaluronan biosynthesis. **International Journal of Biological Macromolecules**, v. 16, n. 6, p. 283–286, 1994.

RINAUDO, M. et al. Effect of Mannitol on Hyaluronic Acid Stability in Two *in Vitro* Models of Oxidative Stress. **Polymers**, v. 6, p. 1948–1957, 2014.

SAMUNI, A. et al. Tempol, a Stable Free Radical, Is a Novel Murine Radiation Protector. **Cancer Research**, v. 52, n. 7, p. 1750–1753, 1992.

SANNINO, A. et al. Cellulose derivative-hyaluronic acid-based microporous hydrogels cross-linked through divinyl sulfone (DVS) to modulate equilibrium sorption capacity and network stability. **Biomacromolecules**, v. 5, n. 1, p. 92–96, 2004.

SCHNACKENBERG, C. G. Physiological and pathophysiological roles of oxygen radicals in the renal microvasculature. **American Journal of Physiology-Regulatory, Integrative and Comparative Physiology**, v. 282, p. R335–R342, 2002.

SHEU, S. Y. et al. Biological characterization of oxidized hyaluronic acid/resveratrol hydrogel for cartilage tissue engineering. **Journal of Biomedical Materials Research - Part A**, v. 101, n. 12, p. 3457–3466, 2013.

SHIMOJO, A. A. M. et al. The performance of crosslinking with divinyl sulfone as controlled by the interplay between the chemical modification and conformation of hyaluronic acid. **Journal of the Brazilian Chemical Society**, v. 26, n. 3, p. 506–512, 2015.

SHOHAM, N. et al. The mechanics of hyaluronic acid/adipic acid dihydrazide hydrogel: Towards developing a vessel for delivery of preadipocytes to native tissues. **Journal of the Mechanical Behavior of Biomedical Materials**, v. 28, p. 320–331, 2013.

ŠOLTÉS, L. et al. Degradative action of reactive oxygen species on hyaluronan. **Biomacromolecules**, v. 7, n. 3, p. 659–668, 2006.

SU, W. Y.; CHEN, Y. C.; LIN, F. H. Injectable oxidized hyaluronic acid/adipic acid dihydrazide hydrogel for nucleus pulposus regeneration. **Acta Biomaterialia**, v. 6, n. 8, p. 3044–3055, 2010.

TAN, H. et al. Injectable *in situ* forming biodegradable chitosan-hyaluronic acid based hydrogels for cartilage tissue engineering. **Biomaterials**, v. 30, n. 13, p. 2499–2506, 2009.

TEZEL, A.; FREDRICKSON, G. H. The science of hyaluronic acid dermal fillers. **Journal of Cosmetic and Laser Therapy**, v. 10, p. 35–42, 2008.

THIEMERMANN, C. Membrane-permeable radical scavengers (tempol) for shock, ischemia-reperfusion injury, and inflammation. **Crit Care Med.**, v. 31, n. 0090-3493, p. S76–S84, 2003.

UTHMAN, I.; RAYNAULD, J.-P.; HARAOUI, B. Intra-articular therapy in osteoarthritis. **Postgraduate Medical Journal**, v. 79, n. 934, p. 449–453, 2003.

VALAVANIDIS, A. et al. Comparison of the Radical Scavenging Potential of Polar and Lipidic Fractions of Olive Oil and Other Vegetable Oils under Normal Conditions and after Thermal Treatment. **Journal of Agricultural and Food Chemistry**, v. 52, n. 8, p. 2358–2365, 2004.

WATTERSON, J.; ESDAILE, J. Viscosupplementation: therapeutic mechanisms and clinical

potential in osteoarthritis of the knee. **Journal of the American Academy of Orthopaedic Surgeons**, v. 8, n. 277–284, 2000.

WEIS, M. et al. Evaluation of Hydrogels Based on Oxidized Hyaluronic Acid for Bioprinting. **Gels**, v. 4, n. 4, p. 82, 2018.

WILCOX, C. S.; PEARLMAN, A. Chemistry and antihypertensive effects of tempol and other nitroxides. **Pharmacological reviews**, v. 60, n. 4, p. 418–469, 2008.

WU, X. et al. Interleukin-6 from subchondral bone mesenchymal stem cells contributes to the pathological phenotypes of experimental osteoarthritis. **American Journal of Translational Research**, v. 10, n. 4, p. 1143–1154, 2018.

YEN, G. C.; CHEN, H. Y. Antioxidant Activity of Various Tea Extracts in Relation to Their Antimutagenicity. **Journal of Agricultural and Food Chemistry**, v. 43, n. 1, p. 27–32, 1995.